Bulletin of the Earthquake
Research Institute
Vol. 44 (1966), pp. 179-213

11. *Magnetization of Four Pacific Seamounts near the Japanese Islands.*

By Seiya Uyeda,*

Earthquake Research Institute and Geophysical Institute

and

Michael Richards,

Scripps Institution of Oceanography, University of California, San Diego.

(Read Sept. 28, 1965.—Received Dec. 22, 1965.)

Abstract

The direction and magnitude of the magnetization of four seamounts in the Pacific near the Japanese Islands are computed, using the total magnetic force and topographic survey data reported previously (Uyeda *et al.*, *Bull. Earthq. Res. Inst.*, 42, 555-570, 1964). Computation is made following Vacquier's method in which uniform magnetization is assumed. The results indicate that these seamounts are magnetized normally in declination but much shallower or reversed in inclination compared with the present geomagnetic field. Depending on the relative intensity of induced magnetization and remanent magnetization, the estimated palaeomagnetic pole positions fall in the central to north Atlantic Ocean. Some Cretaceous index fossils were reported from one of the seamounts. Some speculations are made regarding the possible significance of the obtained pole positions on the movements of ocean floors.

1. Introduction

A machine method for computing the magnitude and direction of magnetization of a uniformly magnetized body from shape and a magnetic survey was developed by *V. Vacquier* (1962). A program** written for a CDC 3600 computer by one of us (M.R.) along Vacquier's method was revised by S. U. for an IBM 7090 computer to compute the magnetization

* Computations were made by an IBM 7090 computer at the Computation Center of Stanford University in 1965, while the author was at the Department of Geophysics, Stanford University on leave from the University of Tokyo.

** G. Van Voorhis of the U. S. Naval Oceanographic Office wrote a part of the original program for the CDC 1604.

of four seamounts in the northwestern Pacific near the Japanese Islands. The magnetic survey over these seamounts was made by a proton-precession magnetometer during the cruises of Japanese Expedition of Deep Seas (JEDS IV, VI, VII, and VIII cruises). The results of the surveys were published elsewhere (*Uyeda et al.*, 1962; *Uyeda et al.*, 1964).

In Vacquier's method, the total magnetic intensity anomaly ΔT is expressed as the sum of the projections of the horizontal anomaly ΔH and of the vertical anomaly ΔZ in the direction of the total geomagnetic field:

$$\Delta T = \Delta H \cos i + \Delta Z \sin i \qquad (1)$$

where i is the magnetic dip, which is assumed to be constant in the area concerned. H is positive toward the magnetic north and Z is positive downward. The mountain body is divided into rectangular prisms of finite size and the sum of the magnetic effect of these prisms is

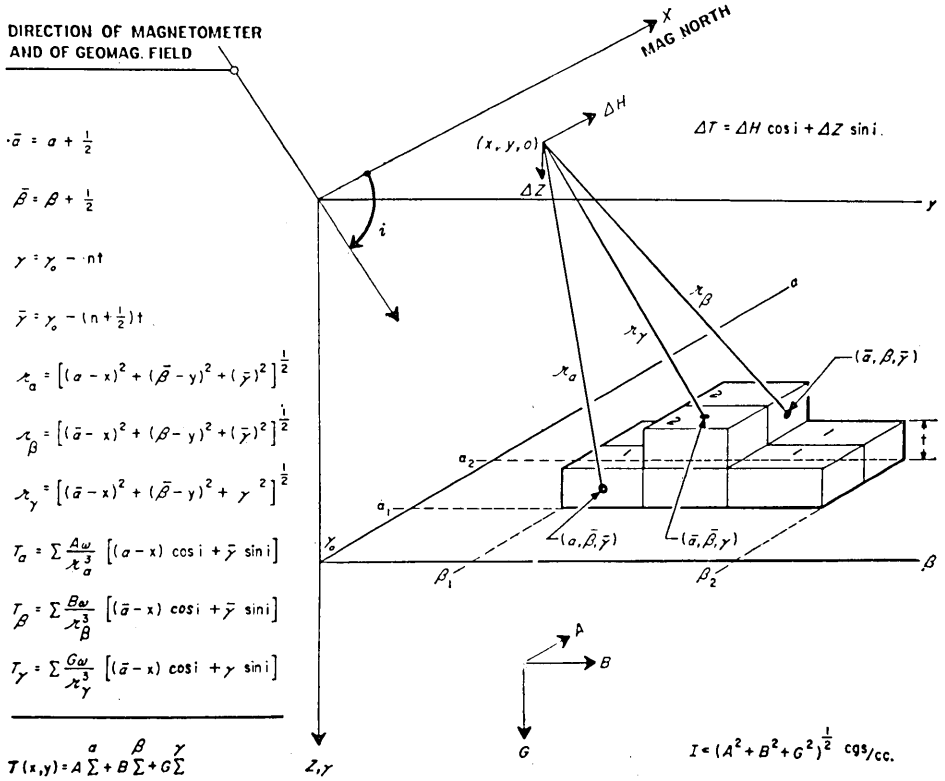

Fig. 1. Diagram of the scheme of computation (taken from *Vacquier*, 1962).

computed. Since the magnetization is assumed uniform, the magnetic effect of the volume magnetization can be replaced by that of free poles on the surfaces of the body. Then, taking the coordinate system as shown in Fig. 1, the total intensity anomalies at $(x, y, 0)$ due to the three categories of surfaces parallel to X, Y and Z axes can be expressed respectively as,

$$T_\alpha(x, y)=A\sum^{\alpha}\frac{\omega}{r_\alpha^3}[(\alpha-x)\cos i+\bar{\gamma}\sin i]\equiv A\sum^{\alpha}(x, y) \tag{2}$$

$$T_\beta(x, y)=B\sum^{\beta}\frac{\omega}{\gamma_\beta^3}[(\bar{\alpha}-x)\cos i+\bar{\gamma}\sin i]\equiv B\sum^{\beta}(x, y) \tag{3}$$

$$T_\gamma(x, y)=G\sum^{\gamma}\frac{\omega}{\gamma_\gamma^3}[(\bar{\alpha}-x)\cos i+\gamma\sin i]\equiv G\sum^{\gamma}(x, y) \tag{4}$$

where A, B and G are northerly, easterly and vertical components of magnetization. ω takes either of the values $+1$ and -1 depending on whether the exterior normal to the prism surface is parallel or antiparallel to the coordinate axes. Then, the total anomaly at $(x, y, 0)$, being the sum of T_α, T_β and T_γ, can be written as

$$T(x, y)=A\sum^{\alpha}(x, y)+B\sum^{\beta}(x, y)+G\sum^{\gamma}(x, y) \tag{5}$$

If the survey was made at n-points on the surface of the sea $(z=0)$, there will be n equations like (5) as

$$\left.\begin{aligned}
T(x_1, y_1)&=A\sum^{\alpha}(x_1, y_1)+B\sum^{\beta}(x_1, y_1)+G\sum^{\gamma}(x_1, y_1)\\
T(x_2, y_2)&=A\sum^{\alpha}(x_2, y_2)+B\sum^{\beta}(x_2, y_2)+G\sum^{\gamma}(x_2, y_2)\\
T(x_3, y_3)&=A\sum^{\alpha}(x_3, y_3)+B\sum^{\beta}(x_3, y_3)+G\sum^{\gamma}(x_3, y_3)\\
&\cdots\quad\cdots\\
T(x_n, y_n)&=A\sum^{\alpha}(x_n, y_n)+B\sum^{\beta}(x_n, y_n)+G\sum^{\gamma}(x_n, y_n)
\end{aligned}\right\} \tag{6}$$

Now, in the equations (6), $T(x_i, y_i)$ are the observed anomaly and $\sum^{\alpha}(x_i, y_i)$, $\sum^{\beta}(x_i, y_i)$ and $\sum^{\gamma}(x_i, y_i)$ are computed from topographic survey data. The unknowns A, B and G can be solved by the method of least squares. In the actual computation, $\sum$'s are first computed and then the normal equations of the least square method

$$\begin{vmatrix} \sum^{n}\left(T\cdot\sum^{\alpha}\right) \\ \sum^{n}\left(T\cdot\sum^{\beta}\right) \\ \sum^{n}\left(T\cdot\sum^{\gamma}\right) \end{vmatrix} = \begin{vmatrix} \left(\sum^{\alpha}\right)^{2} & \left(\sum^{\alpha}\cdot\sum^{\beta}\right) & \left(\sum^{\alpha}\cdot\sum^{\gamma}\right) \\ \left(\sum^{\alpha}\cdot\sum^{\beta}\right) & \left(\sum^{\beta}\right)^{2} & \left(\sum^{\beta}\cdot\sum^{\gamma}\right) \\ \left(\sum^{\alpha}\cdot\sum^{\gamma}\right) & \left(\sum^{\beta}\cdot\sum^{\gamma}\right) & \left(\sum^{\gamma}\right)^{2} \end{vmatrix} \begin{vmatrix} A \\ B \\ G \end{vmatrix} \tag{7}$$

are solved by matrix inversion. With A, B and G, the declination relative to the magnetic north, the inclination and the intensity of magnetization are expressed as

$$D_m = \tan^{-1}(B/A) \tag{8}$$

$$i = \tan^{-1} G/(A^2+B^2)^{1/2} \tag{9}$$

$$I = (A^2+B^2+G^2)^{1/2}\,. \tag{10}$$

Using thus determined values of A, B and G, the magnetic anomaly is reproduced by equations (6). This is called the *computed anomaly*. The difference between the observed anomaly and the computed anomaly is defined as the *residual*. These quantities are plotted by the machine. Then, the means of the absolute values of observed anomaly and residual are computed. Their ratio R is a measure of goodness of the computation.

With the knowledge of the direction of magnetization, the positions of palaeomagnetic virtual poles are calculated. In this calculation, seamounts are assumed to be magnetized only permanently. This is obviously a wrong assumption and the role of possible induced magnetization is discussed in a later section.

2. Data and Computation

The magnetic survey data are all taken from an earlier publication (*Uyeda et al.* 1964). A list of the seamounts studied is in Table I., and their positions are shown in Fig. 2.

In the earlier work, the anomaly charts associated with seamounts were drawn after subtracting the regional trend graphically as reproduced in Figs. 3a, 4a, 5a and 6a. The bathymetric charts are also reproduced in Figs. 3b, 4b, 5b, and 6b. Anomaly values in the unit of gamma at every other mesh point (X, Y) were read from the magnetic charts as shown in Fig. 7a. The length of the side of a square mesh, HU was chosen rather arbitrarily. Then, bathymetry was digitized by assigning

Table I. Seamounts studied and the units of length used in computations.

Seamount	Latitude	Longitude	Present field		Top depth	Bottom depth	Vertical unit, VU,	Horizontal unit, HU,	$DG = HU/VU$
			Local declination	Local inclination					
A	41°16′N	145°58′E	−7.5°	54.0°	2600m	5600m	200m	1480m	7.40
Sisoev	40°55′N	144°54′E	−7.1°	54.0°	3700m	6000m	200m	2065m	10.32
B	40°38′N	146°51′E	−7.0°	53.3°	1400m	5000m	200m	1480m	7.40
Ryofu	38°00′N	145°58′E	−5.1°	50.9°	3000m	5200m	200m	1464m	7.32

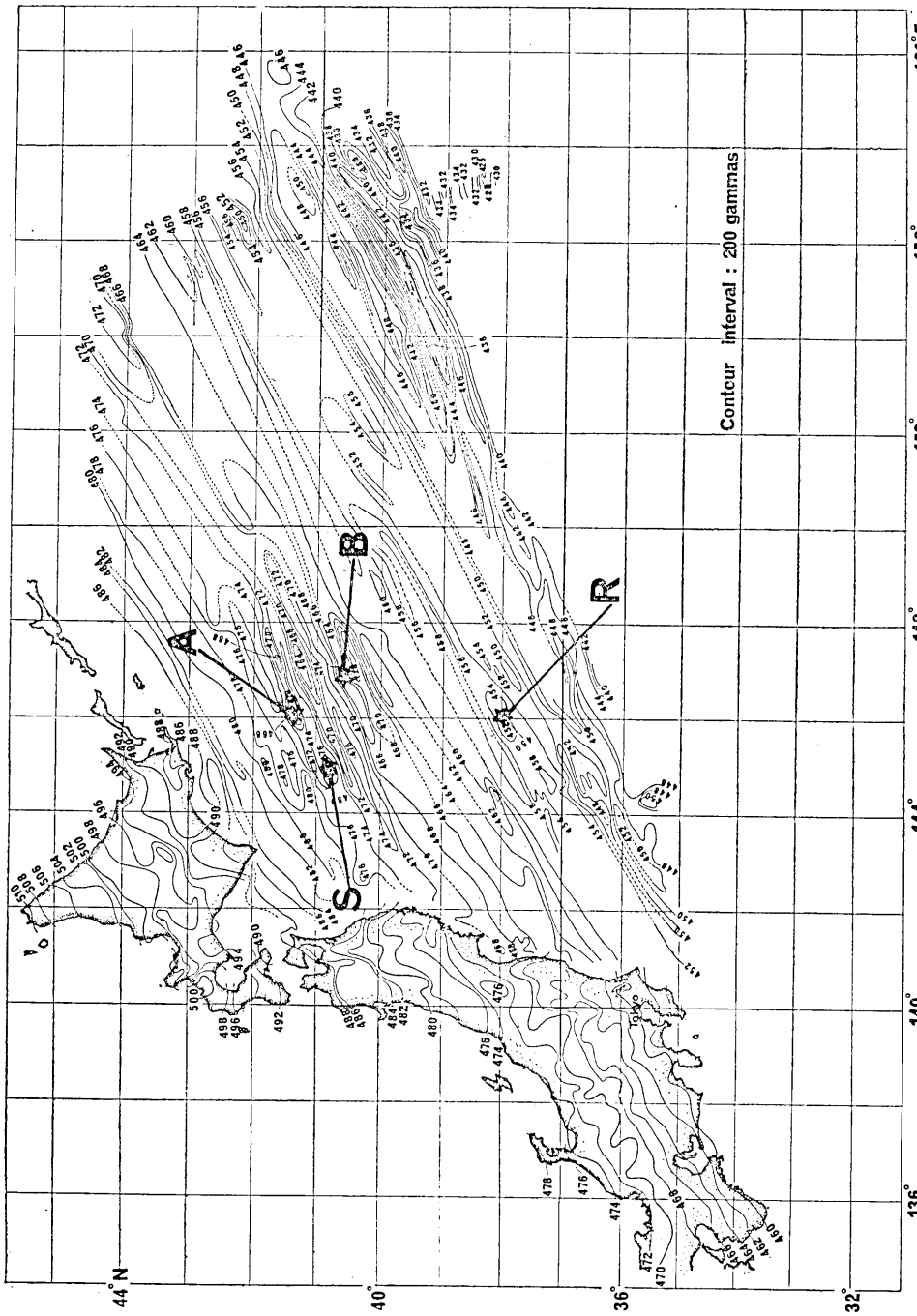

Fig. 2. Positions of seamounts studied, indicated on a chart of total magnetic force of the area (base map taken from *Uyeda et al.*, 1964).

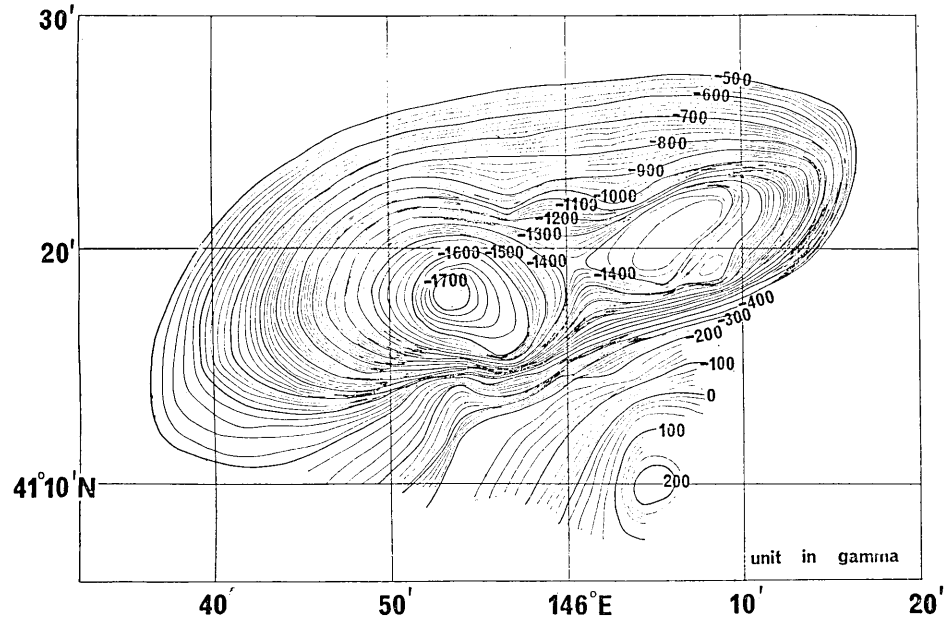

Fig. 3a. Total magnetic force anomally of seamount A (taken from *Uyeda et al.*, 1964).

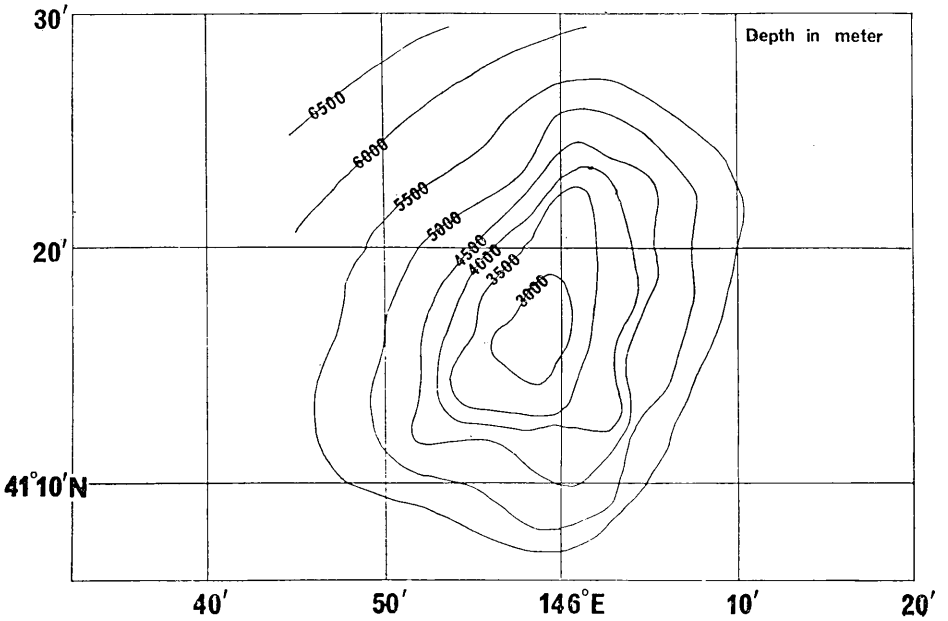

Fig. 3b. Bottom topography of seamount A (taken from *Uyeda et al.*, 1964).

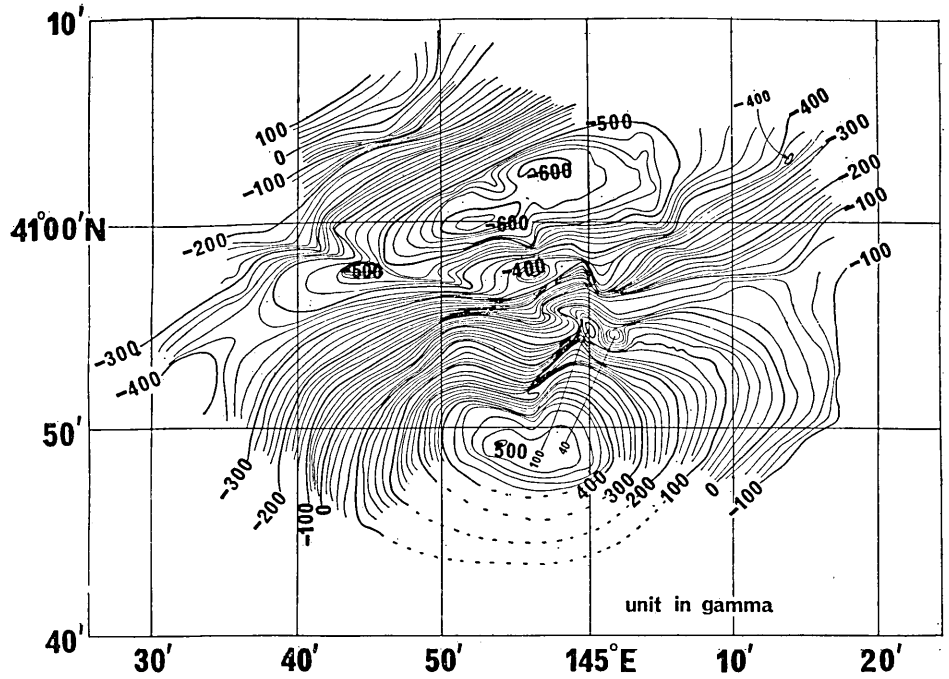

Fig. 4a. Total magnetic force anomaly of seamount Sisoev (taken from *Uyeda et al.*, 1964).

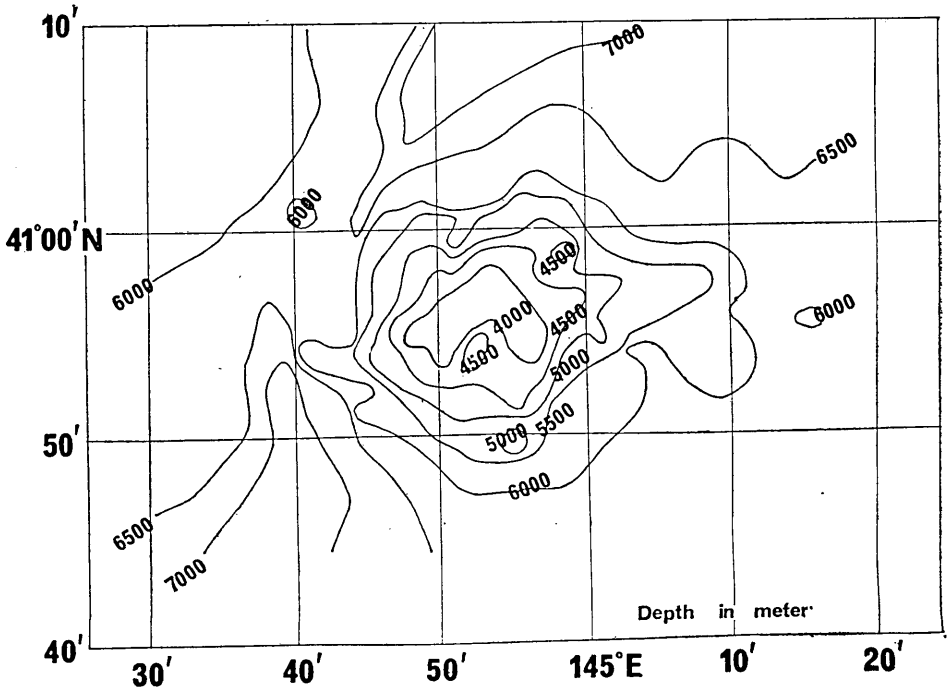

Fig. 4b. Bottom topography of seamount Sisoev (taken from *Uyeda et al.*, 1964).

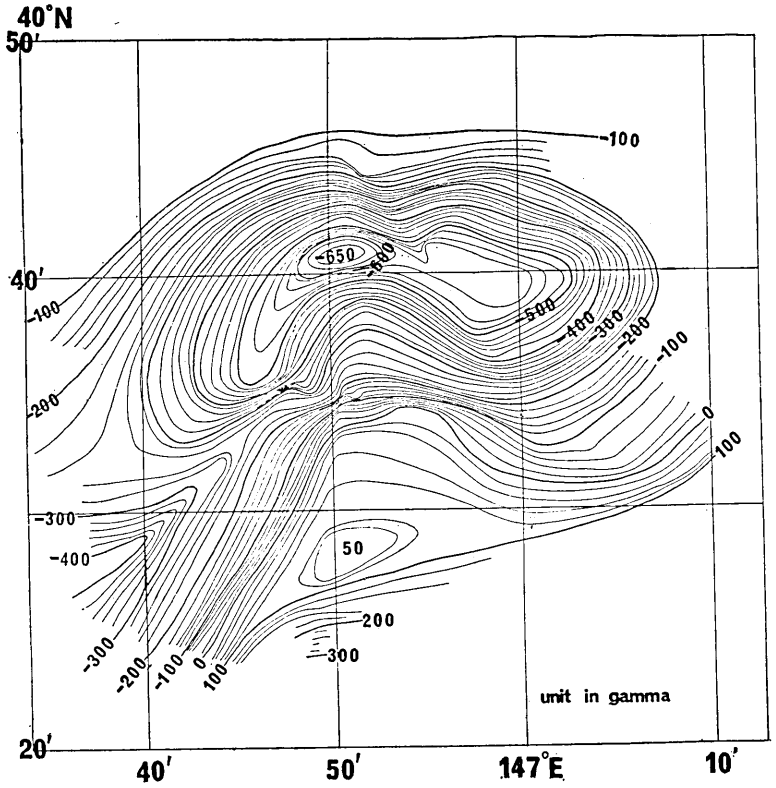

Fig. 5a. Total magnetic force anomaly of seamount B (taken from *Uyeda et al.*, 1964).

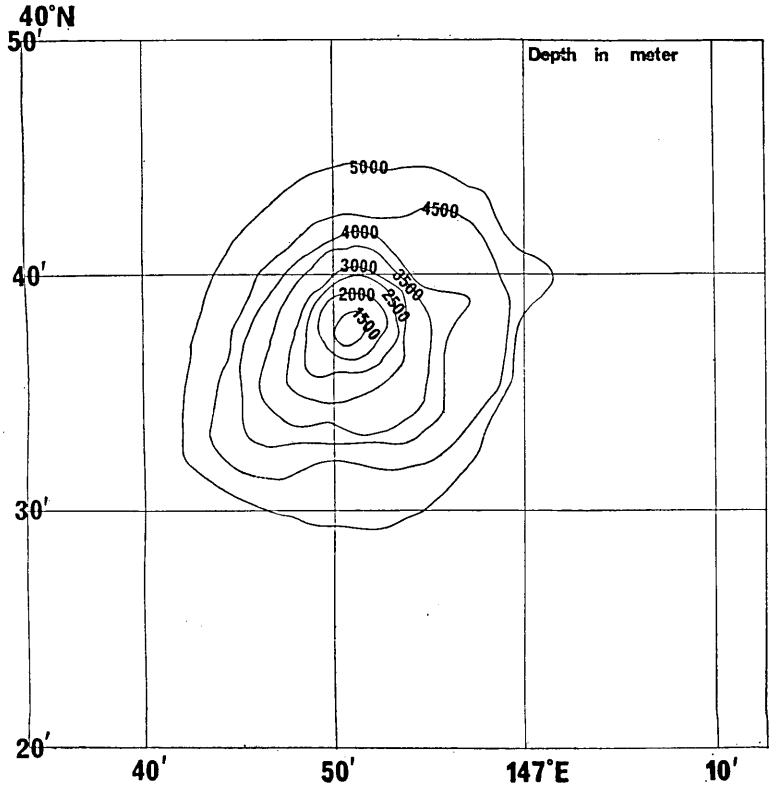

Fig. 5b. Bottom topography of seamount B (taken from *Uyeda et al.*, 1964).

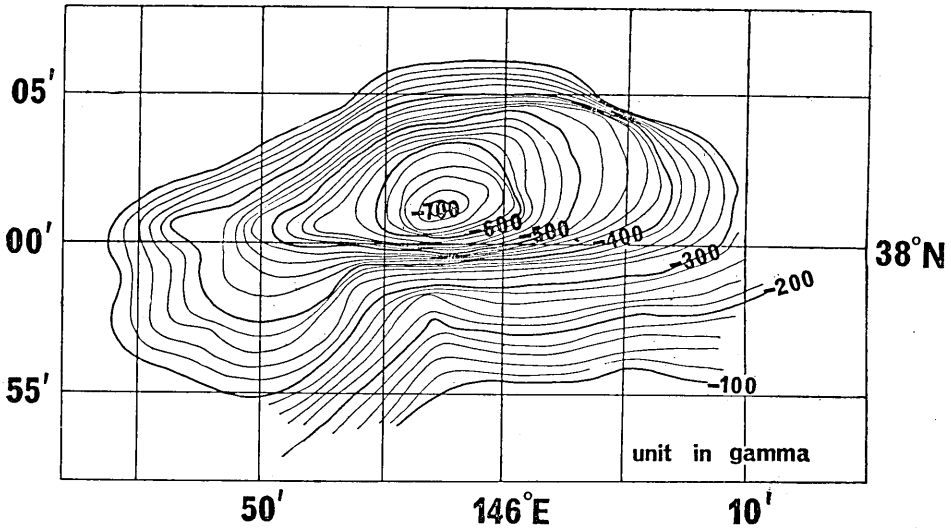

Fig. 6a. Total magnetic force anomaly of seamount Ryofu (taken from *Uyeda et al.*, 1964).

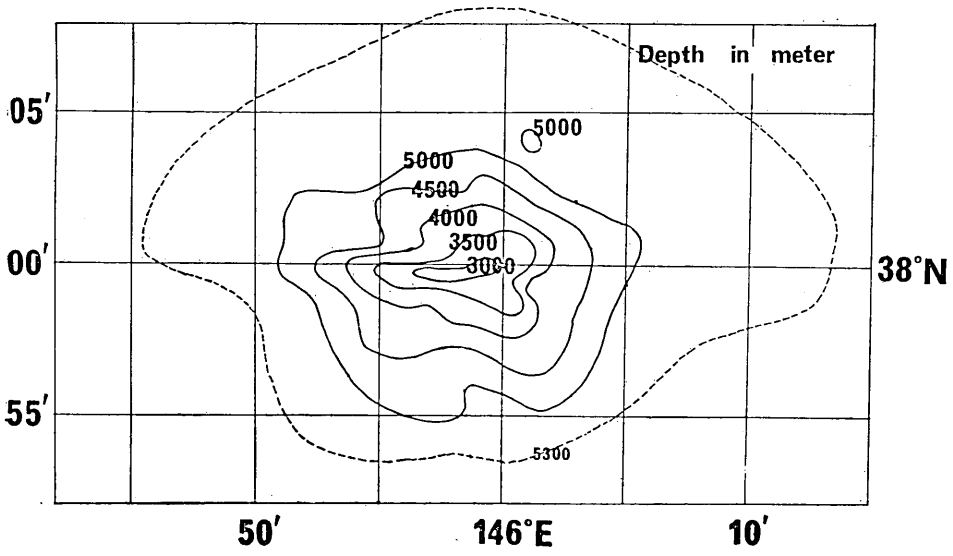

Fig. 6b. Bottom topography of seamount Ryofu (taken from *Uyeda et al.*, 1964).

RYOFU MOUN T

IY= \ IX=	5	6	7	8	9	10	11	12	13	14	15	16	17
1				-310		-300							
2													
3		-320		-362		-357		-360					
4													
5		-350		-405		-410		-390					
6													
7	-300	-370		-418		-470		-430		-310			
8													
9	-250	-345		-410		-500		-490		-370			
10													
11	-195	-270		-350		-530		-570		-450			
12													
13	-153	-270		-310		-600		-630		-530		-360	
14													
15	-117	-207		-320		-630		-670		-560		-378	
16													
17	-130	-228		-327		-580		-660		-558		-380	
18													
19	-140	-230		-327		-520		-540		-510		-350	
20													
21	-120	-215		-320		-470		-488		-470			
22													
23	-128	-210		-317		-420		-445		-320			
24													
25	-138	-220		-300		-350		-350					
26													
27		-200											

Fig. 7a. Example of digitized magnetic anomaly (Seamount Ryofu).

BASE LEVEL = 26

BATHYMETRY

26	26	26	26	26	26	26	26	25	26	26	25	26	26	26	26	26	26	26	26	
26	26	26	26	26	25	25	25	24	24	25	25	25	24	25	25	26	26	26	26	26
26	26	26	25	25	25	24	24	23	23	25	24	23	23	24	25	25	25	26	26	26
26	26	26	26	25	24	23	23	23	23	23	22	21	21	23	24	25	25	25	26	26
26	26	26	25	25	24	22	21	20	19	18	17	17	20	21	23	24	25	25	25	25
26	26	26	25	25	24	22	21	20	19	18	17	17	20	21	23	24	25	25	25	25
26	26	26	25	24	23	20	19	18	17	16	16	17	20	21	22	24	25	25	25	25
26	26	25	25	23	21	19	17	17	16	15	15	16	17	21	22	23	24	25	25	25
26	25	25	24	23	23	22	22	21	19	18	17	18	20	21	23	24	25	25	25	25
25	25	25	25	24	24	23	22	21	20	20	19	20	22	24	25	25	25	25	25	25
25	25	25	25	25	24	24	23	22	23	23	22	23	24	25	25	25	25	25	25	25
25	25	25	25	25	25	25	25	25	24	24	24	25	25	25	25	25	25	26	26	26
26	26	26	26	25	25	25	25	25	25	25	25	25	25	25	25	25	26	26	26	26
26	26	26	26	26	26	26	26	25	25	25	25	25	25	25	26	26	26	26	26	26
26	26	26	26	26	26	26	26	26	26	25	25	25	26	26	26	26	26	26	26	26

E

N

Fig. 7b. Example of digitized topography (Seamount Ryofu): unit of depth is 200m; unit of horizontal scale is 1464m (See Table I).

a depth value for each square (Fig. 7b), using appropriate vertical unit VU (200m in the present cases). The ratios $HU/VU=DG$ are also listed in Table I.

The program we used had a capability of computing the linear regional trend from a set of data and of subtracting the thus determined trend from the observed data. Therefore, two runs were made for each seamount. In one run, removal of trend was not made, whereas in the other it was made. Results of each computation are summarized in Table II. Generally, the results for the two types of runs differ significantly, and the trend-removal run gave a higher "R" ratio which is

Table II. Results of computation.

Seamount	A	B	G	Geo-magnetic Declination	Geographic Declination	Inclination
A, no trend	2.43×10^{-2}	0.133×10^{-2}	-0.549×10^{-2}	3°07′	−4°23′	−12°42′
A, trend	1.56×10^{-2}	0.770×10^{-4}	0.641×10^{-3}	0°17′	−7°13′	2°21′
Sisoev, no trend	1.33×10^{-2}	-0.156×10^{-2}	0.401×10^{-2}	353°19′	346°13′	16°40′
Sisoev, trend	0.941×10^{-2}	-0.193×10^{-2}	0.393×10^{-2}	348°25′	341°19′	22°14′
B, no trend	0.572×10^{-2}	-0.228×10^{-3}	-0.132×10^{-2}	357°43′	350°43′	−12°59′
B, trend	0.391×10^{-2}	-0.761×10^{-5}	-0.248×10^{-3}	359°54′	352°53′	−3°38′
Ryofu, no trend	1.25×10^{-2}	-0.284×10^{-2}	-0.435×10^{-2}	347°13′	342°07′	−18°45′
Ryofu, trend	0.591×10^{-2}	-0.116×10^{-2}	0.294×10^{-3}	348°57′	343°51′	2°48′

Seamount	Intensity (emu/cc)	Goodness Ratio, R	Mean of Abs. Residual	Mean of Abs. Anomaly	Palaeomagnetic Pole Position	
					Latitude (N)	Longitude (E)
A, no trend	2.50×10^{-2}	1.50	0.527×10^{-2}	0.790×10^{-2}	42°05′	−28°10′
A, trend	1.56×10^{-2}	1.82	0.214×10^{-2}	0.389×10^{-2}	49°23′	−22°55′
Sisoev, no trend	1.40×10^{-2}	1.91	0.140×10^{-2}	0.268×10^{-2}	55°22′	−10°37′
Sisoev, trend	1.04×10^{-2}	2.03	0.958×10^{-3}	0.194×10^{-2}	56°23′	−0°36′
B, no trend	0.588×10^{-2}	1.20	0.202×10^{-2}	0.243×10^{-2}	42°12′	−10°42′
B, trend	0.392×10^{-2}	1.41	0.102×10^{-2}	0.144×10^{-2}	47°04′	−22°41′
Ryofu, no trend	1.35×10^{-2}	1.45	0.255×10^{-2}	0.369×10^{-2}	39°31′	−10°56′
Ryofu, trend	0.603×10^{-2}	2.44	0.402×10^{-3}	0.980×10^{-3}	50°31′	−8°06′

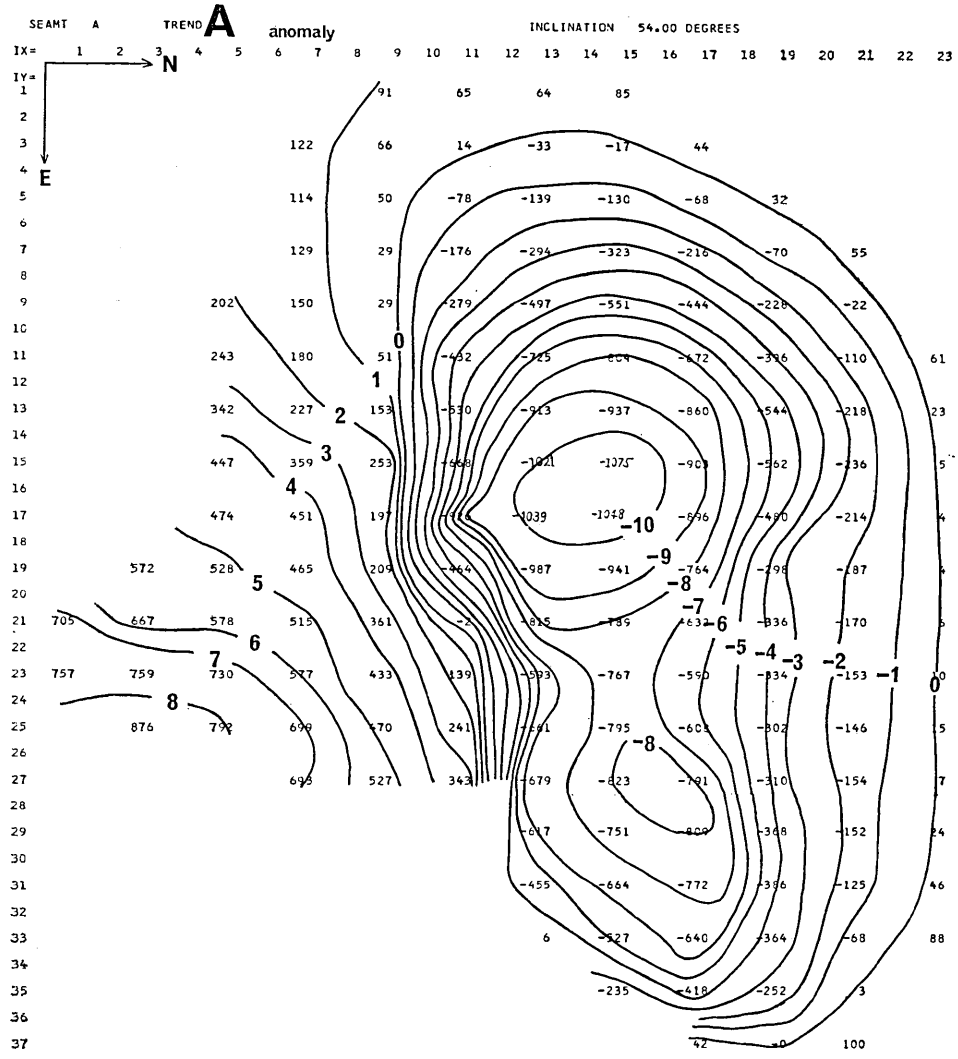

Fig. 8a. Observed magnetic anomaly (trend removed) of seamount A: contour interval $=100\gamma$.

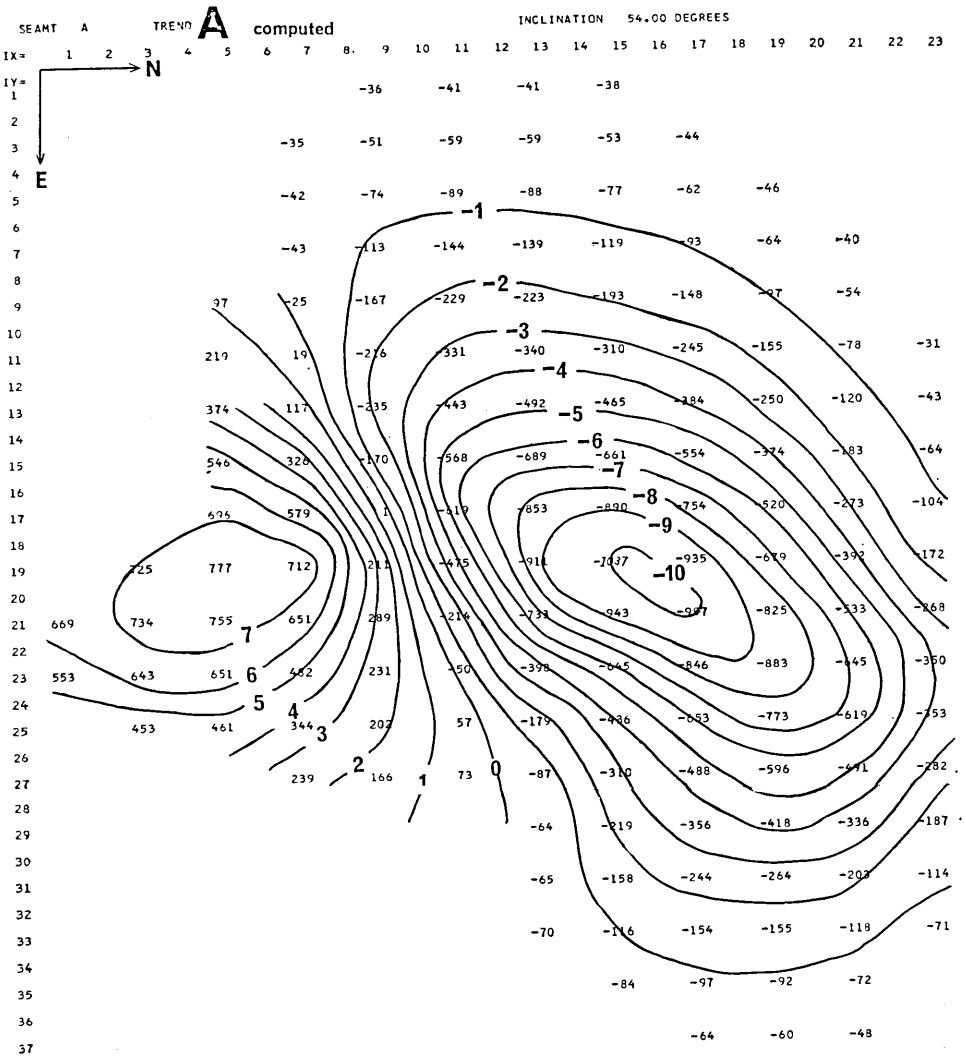

Fig. 8b. Computed magnetic anomaly of seamount A. contour interval $=100\gamma$.

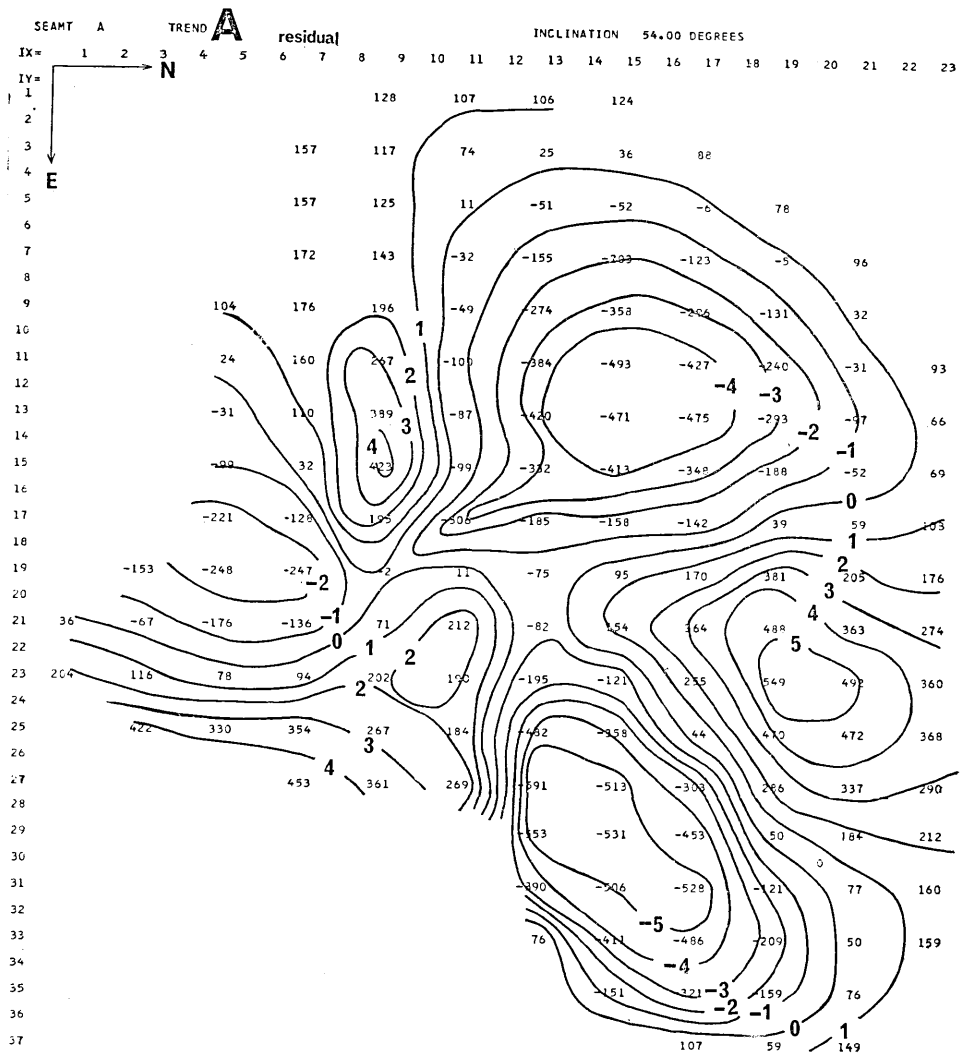

Fig. 8c. Residual field of seamount A: contour interval $=100\gamma$.

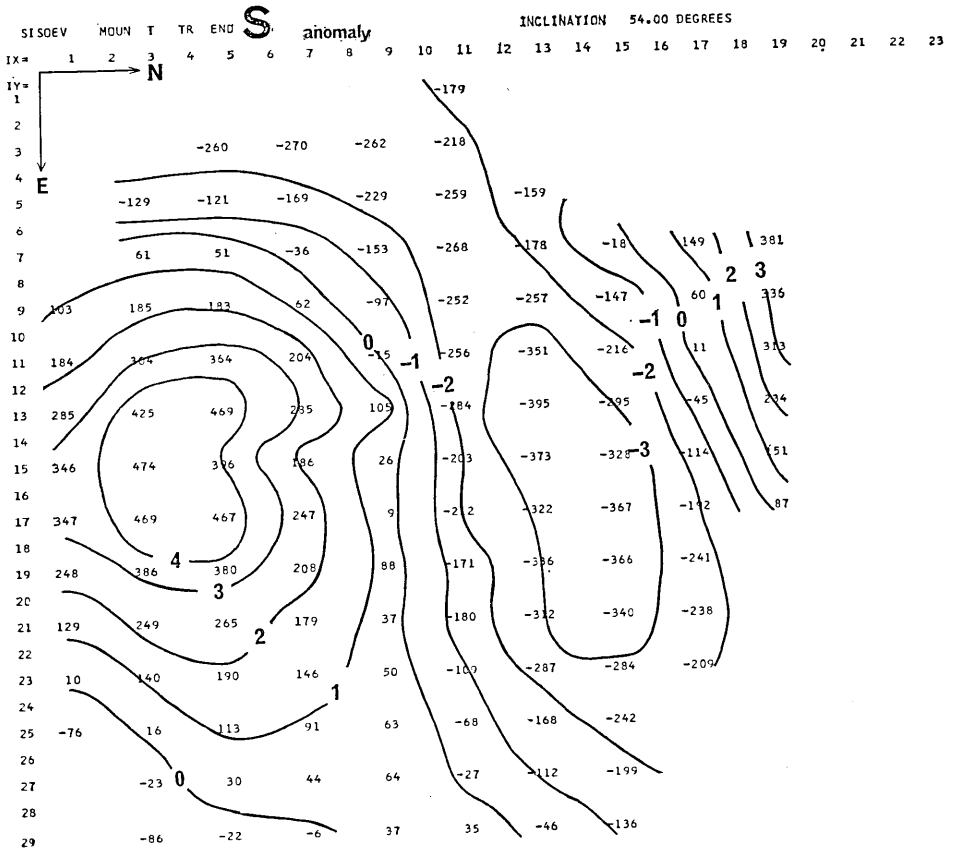

Fig. 9a. Observed magnetic anomaly (trend removed) of seamount Sisoev: contour interval $=100\gamma$.

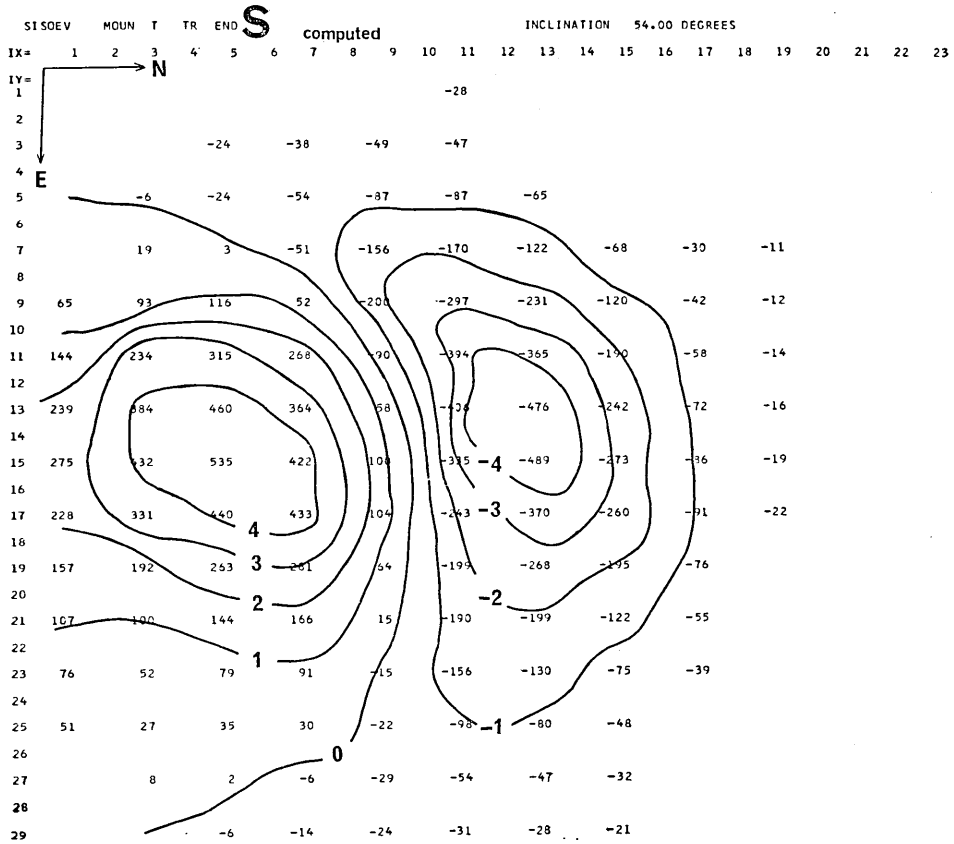

Fig. 9b. Computed magnetic anomaly of seamount Sisoev: contour interval $=100\gamma$.

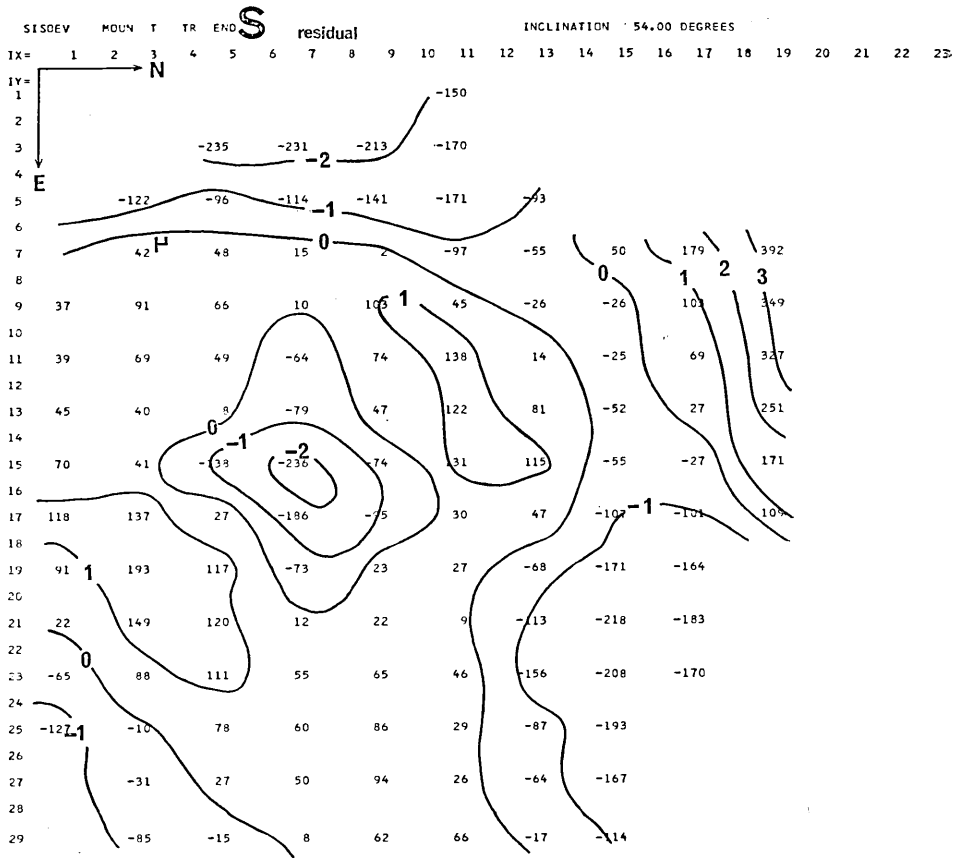

Fig. 9c. Residual field of seamount Sisoev: contour interval $=100\gamma$.

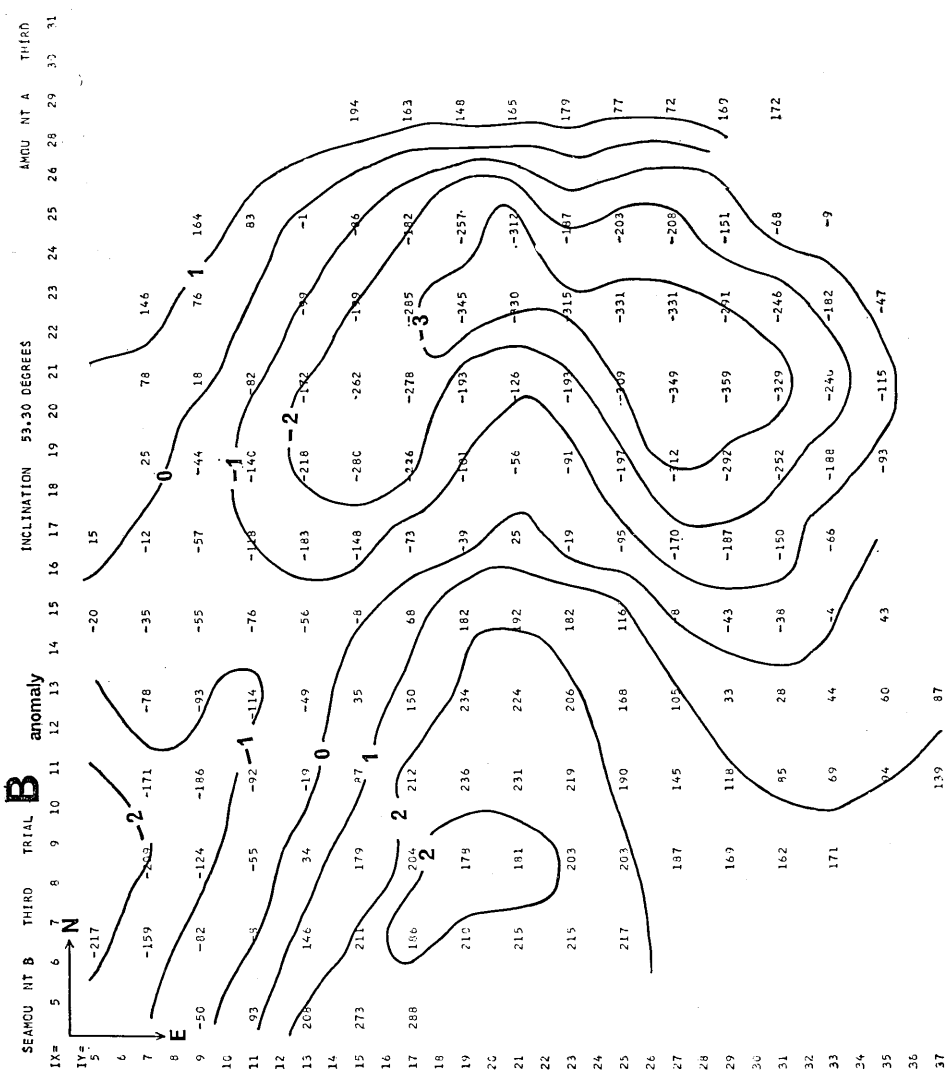

Fig. 10a. Observed magnetic anomaly (trend removed) of seamount B: contour interval =100γ

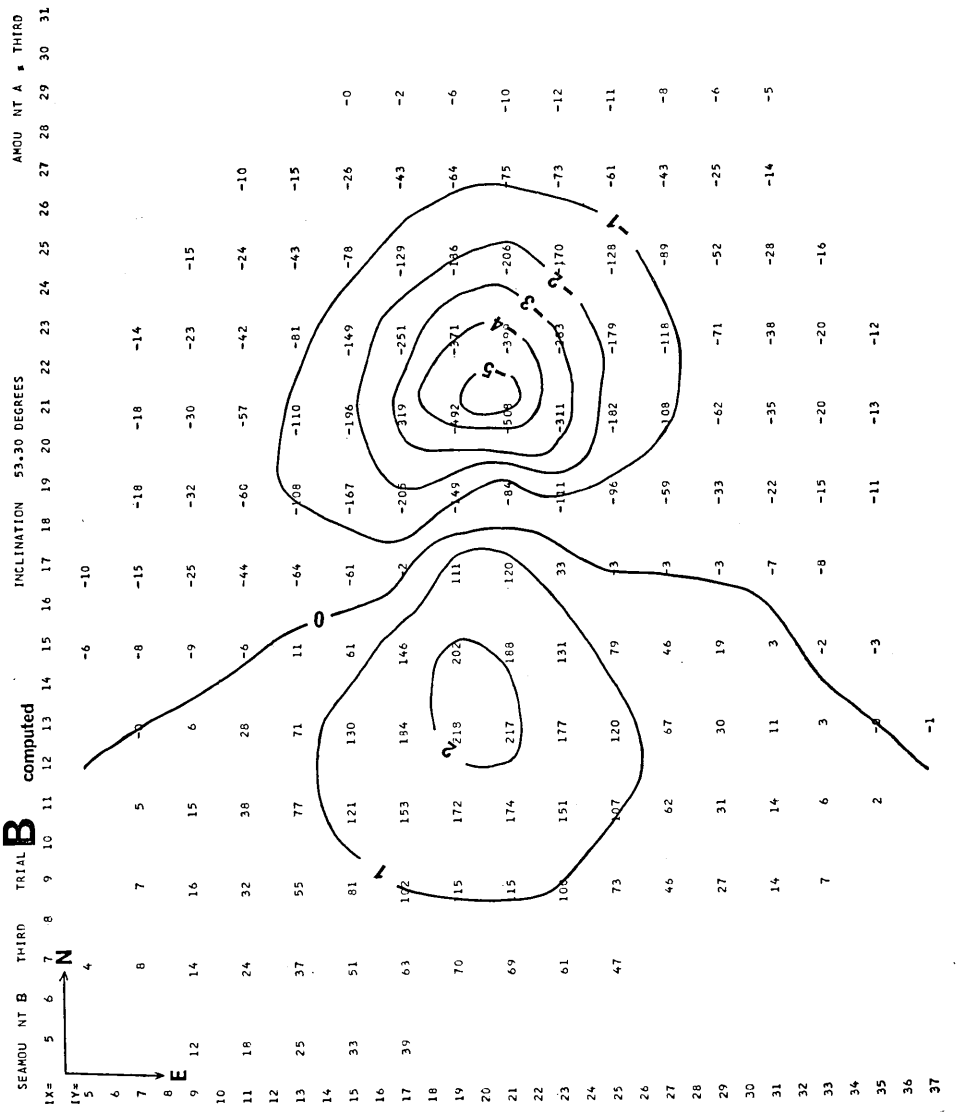

Fig. 10b. Computed magnetic anomaly of seamount B: contour interval =100γ.

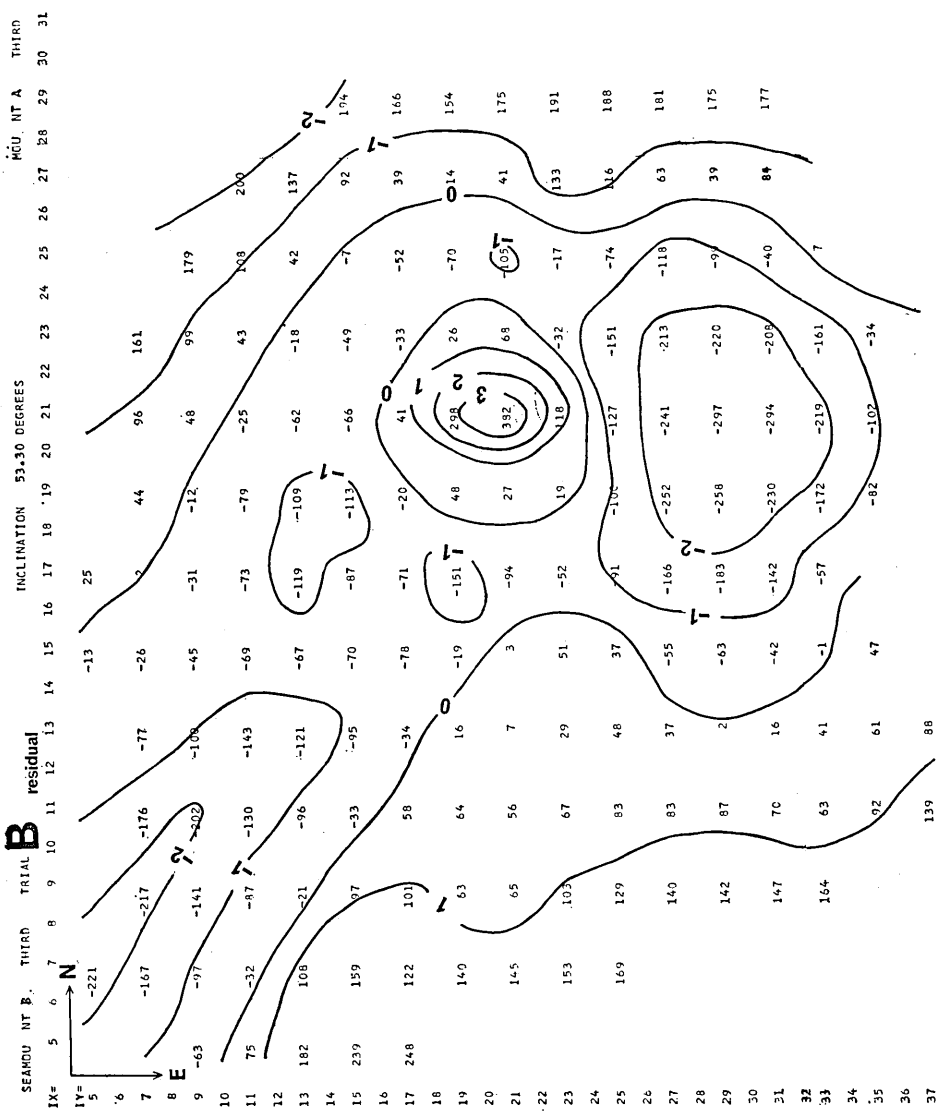

Fig. 10c. Residual field of seamount B: contour interval =100γ.

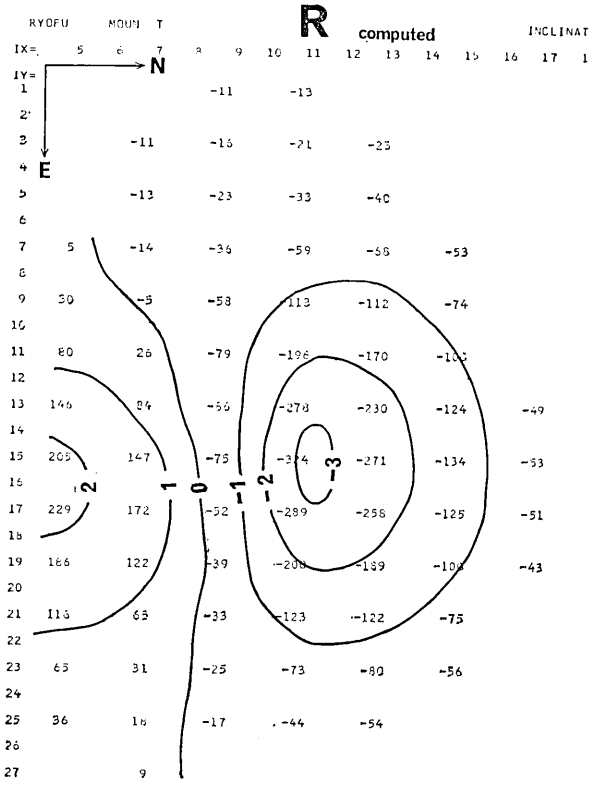

Fig. 11b. Computed magnetic anomaly of seamount Ryofu: contour interval $=100\gamma$.

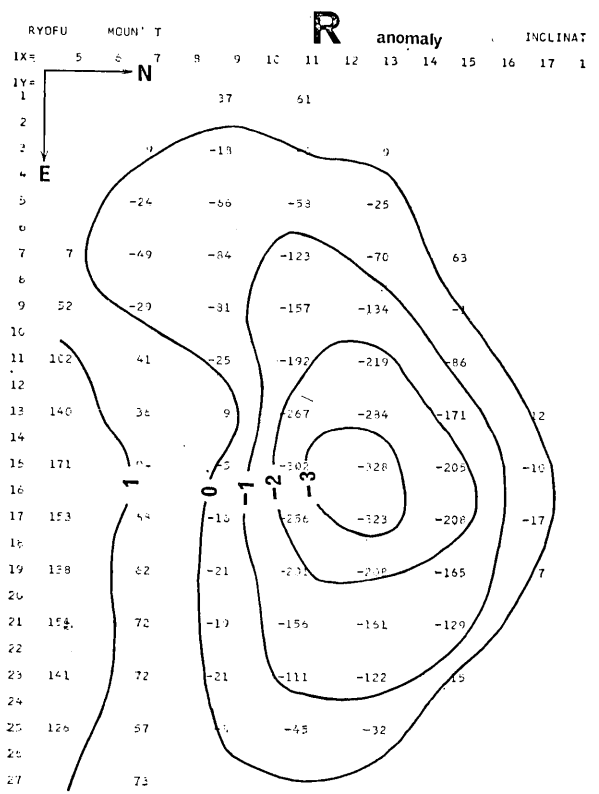

Fig. 11a. Observed magnetic anomally (trend removed) of seamount Ryofu: contour interval $=100\gamma$.

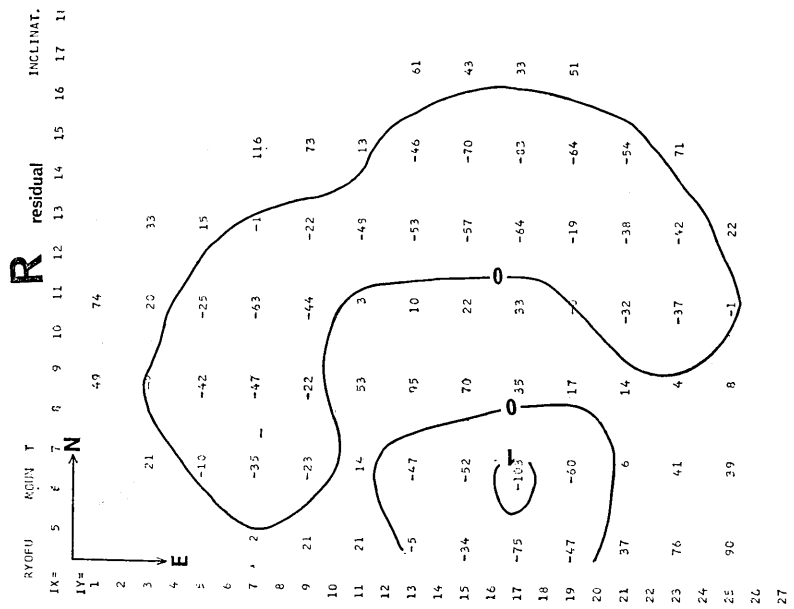

Fig. 11c. Residual field of seamount Ryofu: contour interval $=100\gamma$.

indicative of a better fit of observed and computed values. In the following, therefore, we will disregard the results of the first-type runs. In any case, however, small values of the R-ratio in Table II indicate that very good agreement between the observed anomaly and computed anomaly cannot be expected. Figs. 8 a, b, c, ~11 a, b, c are, for each seamount, the plot of the anomaly after removal of trend, the plot of the computed anomaly and the plot of the residuals, respectively. Comparison of the observed and computed anomalies gives an idea about the degree of closeness of fit. On the whole, the agreement between the two is good only for the general features and many details are not well reproduced.

3. Results and Discussion

It may be observed in Tables I and II that the declinations of magnetization of these seamounts are rather close to both the present geomagnetic and geographic meridians pointing to the north but the inclinations are much shallower than both the actual inclination of the field and that of the theoretical dipole. This brings about the occurrence

Table III. Numerical experiments on Seamount Ryofu.

Case	Declination (geographic)	Inclination	Intensity	Goodness Ratio, R	Palaeomagnetic Pole Position	
					Latitude	Longitude
R: uniform magnetization	343°51′	2°48′	0.603×10^{-2}	2.44	50°31′	−8°06′
1: western half non-magnetic	347°47′	1°35′	0.857×10^{-2}	1.61	51°08′	−14°21′
2: northern half non-magnetic	337°32′	20°12′	0.562×10^{-2}	1.88	55°51′	7°59′
3: southern half non-magnetic	334°30′	−53°25′	0.679×10^{-2}	2.07	16°36′	20°40′
4: eastern half non-magnetic	351°42′	−3°52′	0.788×10^{-2}	1.56	49°20′	−21°16′
5: central part non-magnetic	339°02′	−11°04′	1.21×10^{-2}	1.43	42°16′	−5°17′
6: top half non-magnetic	343°11′	2°13′	0.943×10^{-2}	3.36	50°00′	−7°17′
7: outer half non-magnetic	346°39′	−0°02′	0.586×10^{-2}	1.76	50°02′	−12°58′
8: NS alternation	343°30′	2°02′	1.23×10^{-2}	2.48	50°02′	−7°56′
9: EW alternation	345°30′	2°00′	1.34×10^{-2}	2.54	50°40′	−10°47′

of palaeomagnetic pole positions in the North Atlantic as shown in Fig. 12. Closeness of the obtained palaeomagnetic pole positions, in spite of the uncertainties involved in the computations, is remarkable.

Here, a set of numerical experiments were conducted to see the scatter in the pole positions due to possible non-uniform magnetization of the seamounts. The seamount Ryofu was chosen for the experiments. Maintaining the assumption of uniformity in the direction of magnetization, we assumed that various parts of the mountain body were non magnetic and examined the shifts of pole positions due to such a non-uniformity. These assumptions correspond to the extreme cases of non-uniformly distributed intensity of magnetization. First, it was assumed that the western half of the mountain body was non-magnetic. Computationwise, this case is treated by taking the topography as shown in Fig. 13-1, instead of Fig. 7b: in Fig. 13-1, the depth of the western half of the seamount is taken to be equal to the depth of the base of the mountain. The numerical results and the pole position obtained are shown in Table III and in Fig. 14. It may be observed that the pole position is shifted about 10 degrees to the west and the goodness ratio, R, became 1.61 as compared with 2.44 in the case of uniform magnetization. Similar calculations for eight different types of assumed non-uniformity were made. Topographies changed according to the assumed non-uniform

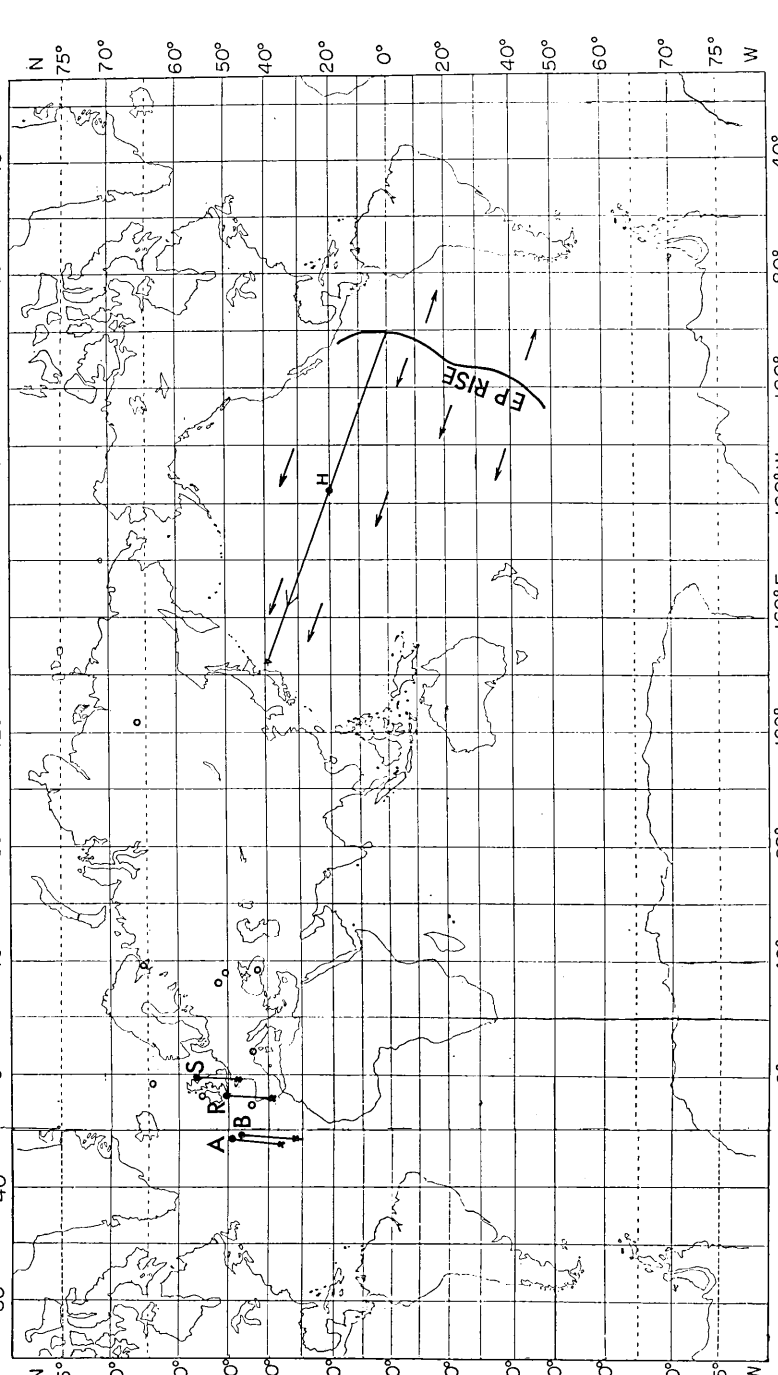

Fig. 12. Palaeomagnetic pole positions for the seamounts. Arc segments attached to each pole positions are the possible shifts of pole positions due to the induced component of magnetization. The arcs end when the ratio of remanent to induced magnetizations (Q-ratio) is 2. Open circles are for the Hawaiian seamounts computed by *Richards, Vacquier and van Voorhis*, (1965). Arrows in the Pacific basin are the direction of the spreading of the basin according to *J. T. Wilson* (1963).

BASE LEVEL = 26

BATHYMETRY

26	26	26	26	26	26	26	26	26	26	26	26	25	26	26	26	26	26	26	26	26	26
26	26	26	26	26	26	26	26	26	26	26	25	25	24	25	25	26	26	26	26	26	26
26	26	26	26	26	26	26	26	26	26	26	24	23	23	24	25	25	25	26	26	26	26
26	26	26	26	26	26	26	26	26	26	26	22	21	21	23	24	25	25	25	26	26	26
26	26	26	26	26	26	26	26	26	26	26	20	19	20	22	24	25	25	25	25	25	26
26	26	26	26	26	26	26	26	26	26	26	17	17	20	21	23	24	25	25	25	25	25
26	26	26	26	26	26	26	26	26	26	26	16	17	20	21	22	24	25	25	25	25	25
26	26	26	26	26	26	26	26	26	26	26	15	16	17	21	22	23	24	25	25	25	25
26	26	26	26	26	26	26	26	26	26	26	17	18	20	21	23	24	25	25	25	25	25
26	26	26	26	26	26	26	26	26	26	26	19	20	22	24	25	25	25	25	25	25	25
26	26	26	26	26	26	26	26	26	26	26	22	23	24	25	25	25	25	25	25	25	25
26	26	26	26	26	26	26	26	26	26	26	24	25	25	25	25	25	25	26	26	26	26
26	26	26	26	26	26	26	26	26	26	26	25	25	25	25	25	26	26	26	26	26	26
26	26	26	26	26	26	26	26	26	26	26	25	25	25	26	26	26	26	26	26	26	26
26	26	26	26	26	26	26	26	26	26	26	25	25	26	26	26	26	26	26	26	26	26

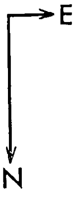

Fig. 13-1. Digitized topography for case 1, where the western half of the seamount Ryofu is assumed non-magnetic. Unit of depth is 200m and the unit of horizontal scale is 1464m.

BASE LEVEL = 26

BATHYMETRY

26	26	26	26	26	26	26	26	25	26	26	26	25	26	26	26	26	26	26	26	26	26
26	26	26	26	26	25	25	25	24	24	25	25	25	24	25	25	26	26	26	26	26	26
26	26	26	25	25	25	24	24	23	23	25	24	23	23	24	25	25	25	26	26	26	26
26	26	26	26	25	24	23	23	23	23	23	22	21	21	23	24	25	25	25	26	26	26
26	26	26	25	25	24	22	22	21	21	21	20	19	20	22	24	25	25	25	25	25	26
26	26	26	25	25	24	22	21	20	19	18	17	17	20	21	23	24	25	25	25	25	25
26	26	26	25	24	23	20	19	18	17	16	16	17	20	21	22	24	25	25	25	25	25
26	26	25	25	23	21	19	17	17	16	15	15	16	17	21	22	23	24	25	25	25	25
26	26	26	26	26	26	26	26	26	26	26	26	26	26	26	26	26	26	26	26	26	26
26	26	26	26	26	26	26	26	26	26	26	26	26	26	26	26	26	26	26	26	26	26
26	26	26	26	26	26	26	26	26	26	26	26	26	26	26	26	26	26	26	26	26	26
26	26	26	26	26	26	26	26	26	26	26	26	26	26	26	26	26	26	26	26	26	26
26	26	26	26	26	26	26	26	26	26	26	26	26	26	26	26	26	26	26	26	26	26
26	26	26	26	26	26	26	26	26	26	26	26	26	26	26	26	26	26	26	26	26	26
26	26	26	26	26	26	26	26	26	26	26	26	26	26	26	26	26	26	26	26	26	26

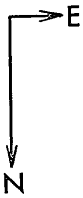

Fig. 13-2. Digitized topography for case 2, where the northern half of the seamount Ryofu is assumed non-magnetic. Units are the same as in Fig. 13-1.

BASE LEVEL = 26

BATHYMETRY

26	26	26	26	26	26	26	26	26	26	26	26	26	26	26	26	26	26	26	26	26	26
26	26	26	26	26	26	26	26	26	26	26	26	26	26	26	26	26	26	26	26	26	26
26	26	26	26	26	26	26	26	26	26	26	26	26	26	26	26	26	26	26	26	26	26
26	26	26	26	26	26	26	26	26	26	26	26	26	26	26	26	26	26	26	26	26	26
26	26	26	26	26	26	26	26	26	26	26	26	26	26	26	26	26	26	26	26	26	26
26	26	26	26	26	26	26	26	26	26	26	26	26	26	26	26	26	26	26	26	26	26
26	26	26	26	26	26	26	26	26	26	26	26	26	26	26	26	26	26	26	26	26	26
26	26	26	26	26	26	26	26	26	26	26	26	26	26	26	26	26	26	26	26	26	26
26	26	25	25	23	21	19	17	17	16	15	15	16	17	21	22	23	24	25	25	25	25
26	25	25	24	23	23	22	22	21	19	18	17	18	20	21	23	24	25	25	25	25	25
25	25	25	25	24	24	23	22	21	20	20	19	20	22	24	25	25	25	25	25	25	25
25	25	25	25	25	25	25	25	25	24	24	24	25	25	25	25	25	25	26	26	26	26
26	26	26	26	25	25	25	25	25	25	25	25	25	25	25	25	26	26	26	26	26	26
26	26	26	26	26	26	26	26	25	25	25	25	25	25	26	26	26	26	26	26	26	26
26	26	26	26	26	26	26	26	26	26	25	25	25	26	26	26	26	26	26	26	26	26

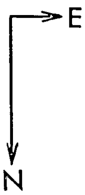

Fig. 13-3. Digitized topography for case 3, where the southern half of the seamount Ryofu is assumed non-magnetic. Units are the same as in Fig. 13-1.

BASE LEVEL = 26

BATHYMETRY

```
26 26 26 26 26 26 26 26 25 26 26 26 26 26 26 26 26 26 26 26 26 26
26 26 26 26 25 25 25 25 24 24 25 26 26 26 26 26 26 26 26 26 26 26
26 26 26 25 25 25 24 24 23 23 25 26 26 26 26 26 26 26 26 26 26 26
26 26 26 25 24 23 23 23 23 23 23 26 26 26 26 26 26 26 26 26 26 26
26 26 26 25 25 24 22 22 21 21 21 26 26 26 26 26 26 26 26 26 26 26
26 26 26 25 25 24 22 21 20 19 18 26 26 26 26 26 26 26 26 26 26 26
26 26 26 25 24 23 20 19 18 17 16 26 26 26 26 26 26 26 26 26 26 26
26 26 25 25 23 21 19 17 17 16 15 26 26 26 26 26 26 26 26 26 26 26
26 25 25 24 23 23 22 22 21 19 18 26 26 26 26 26 26 26 26 26 26 26
25 25 25 25 24 24 23 22 21 20 20 26 26 26 26 26 26 26 26 26 26 26
25 25 25 25 25 24 24 23 22 23 23 26 26 26 26 26 26 26 26 26 26 26
25 25 25 25 25 25 25 25 25 24 24 26 26 26 26 26 26 26 26 26 26 26
26 26 26 26 25 25 25 25 25 25 25 26 26 26 26 26 26 26 26 26 26 26
26 26 26 26 26 26 26 26 25 25 26 26 26 26 26 26 26 26 26 26 26 26
26 26 26 26 26 26 26 26 26 26 25 26 26 26 26 26 26 26 26 26 26 26
```

E

N

Fig. 13-4. Digitized topography for case 4, where the eastern half of the seamount Ryofu is assumed non-magnetic. Units are the same as in Fig. 13-1.

BASE LEVEL = 26

BATHYMETRY

```
26 26 26 26 26 26 26 26 25 26 26 26 25 26 26 26 26 26 26 26 26 26
26 26 26 26 26 25 25 25 24 24 25 25 25 24 25 25 26 26 26 26 26 26
26 26 26 25 25 25 24 24 23 23 25 24 23 23 24 25 25 25 26 26 26 26
26 26 26 26 25 24 23 23 23 23 23 22 21 21 23 24 25 25 25 26 26 26
26 26 26 25 25 24 22 22 21 21 21 26 26 26 22 24 25 25 25 25 25 26
26 26 26 25 25 24 22 21 26 26 26 26 26 26 21 23 24 25 25 25 25 25
26 26 26 25 24 23 26 26 26 26 26 26 26 26 21 22 24 25 25 25 25 25
26 26 25 25 23 21 26 26 26 26 26 26 26 26 21 22 23 24 25 25 25 25
26 25 25 24 23 23 22 22 21 26 26 26 26 26 21 23 24 25 25 25 25 25
25 25 25 25 24 24 23 22 21 26 26 26 26 22 24 25 25 25 25 25 25 25
25 25 25 25 25 24 24 23 22 23 23 22 23 24 25 25 25 25 25 25 25 25
25 25 25 25 25 25 25 25 25 24 24 24 25 25 25 25 25 25 26 26 26 26
26 26 26 26 25 25 25 25 25 25 25 25 25 25 25 25 25 26 26 26 26 26
26 26 26 26 26 26 26 26 25 25 25 25 25 25 25 26 26 26 26 26 26 26
26 26 26 26 26 26 26 26 26 26 25 25 25 26 26 26 26 26 26 26 26 26
```

E

N

Fig. 13-5. Digitized topography for case 5, where the central part of the seamount Ryofu (Depth <4000m) is assumed non-magnetic. Units are the same as in Fig. 13-1.

BASE LEVEL = 26

BATHYMETRY

```
26 26 26 26 26 26 26 26 25 26 26 26 25 26 26 26 26 26 26 26 26 26
26 26 26 26 26 25 25 25 24 24 25 25 25 24 25 25 26 26 26 26 26 26
26 26 26 25 25 25 24 24 23 23 25 24 23 23 24 25 25 25 26 26 26 26
26 26 26 26 25 24 23 23 23 23 23 22 21 21 23 24 25 25 25 26 26 26
26 26 26 25 25 24 22 22 21 21 21 26 26 26 22 24 25 25 25 25 25 26
26 26 26 25 25 24 22 21 26 26 26 26 26 26 21 23 24 25 25 25 25 25
26 26 26 25 24 23 26 26 26 26 26 26 26 26 21 22 24 25 25 25 25 25
26 26 25 25 23 21 26 26 26 26 26 26 26 26 21 22 23 24 25 25 25 25
26 25 25 24 23 23 22 22 21 26 26 26 26 26 21 23 24 25 25 25 25 25
25 25 25 25 24 24 23 22 21 26 26 26 26 22 24 25 25 25 25 25 25 25
25 25 25 25 25 24 24 23 22 23 23 22 23 24 25 25 25 25 25 25 25 25
25 25 25 25 25 25 25 25 25 24 24 24 25 25 25 25 25 25 26 26 26 26
26 26 26 26 25 25 25 25 25 25 25 25 25 25 25 25 25 26 26 26 26 26
26 26 26 26 26 26 26 26 25 25 25 25 25 25 25 26 26 26 26 26 26 26
26 26 26 26 26 26 26 26 26 26 25 25 25 26 26 26 26 26 26 26 26 26
```

E

N

Fig. 13-6. Digitized topography for case 6, where the top half of the seamount Ryofu (Depth <4000m) is assumed non-magnetic. Units are the same as in Fig. 13-1.

BASE LEVEL = 26

BATHYMETRY

```
26 26 26 26 26 26 26 26 26 26 26 26 26 26 26 26 26 26 26 26
26 26 26 26 26 26 26 26 26 26 26 26 26 26 26 26 26 26 26 26
26 26 26 26 26 26 26 26 26 26 26 26 26 26 26 26 26 26 26 26
26 26 26 26 26 26 26 26 26 26 26 26 26 26 26 26 26 26 26 26
26 26 26 26 26 26 26 26 26 26 20 19 20 26 26 26 26 26 26 26
26 26 26 26 26 26 26 26 20 19 18 17 17 20 26 26 26 26 26 26
26 26 26 26 26 26 20 19 18 17 16 16 17 20 26 26 26 26 26 26
26 26 26 26 26 26 19 17 17 16 15 15 16 17 26 26 26 26 26 26
26 26 26 26 26 26 26 26 26 19 18 17 18 20 26 26 26 26 26 26
26 26 26 26 26 26 26 26 26 20 20 19 20 26 26 26 26 26 26 26
26 26 26 26 26 26 26 26 26 26 26 26 26 26 26 26 26 26 26 26
26 26 26 26 26 26 26 26 26 26 26 26 26 26 26 26 26 26 26 26
26 26 26 26 26 26 26 26 26 26 26 26 26 26 26 26 26 26 26 26
26 26 26 26 26 26 26 26 26 26 26 26 26 26 26 26 26 26 26 26
```

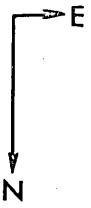

Fig. 13-7. Digitized topography for case 7, where the outer part of the seamount Ryofu (Depth > 4000m) is assumed non-magnetic. Units are the same as in Fig. 13-1.

BASE LEVEL = 26

BATHYMETRY

```
26 26 26 26 26 26 26 26 25 26 26 26 25 26 25 26 26 26 26 26 26 26
26 26 26 26 26 26 25 26 24 26 25 26 25 26 25 26 26 26 26 26 26 26
26 26 26 26 25 26 24 26 23 26 25 26 23 26 24 26 25 26 26 26 26 26
26 26 26 26 25 26 23 26 23 26 23 26 21 26 23 26 25 26 25 26 26 26
26 26 26 26 25 26 22 26 21 26 21 26 19 26 22 26 25 26 25 26 25 26
26 26 26 26 25 26 22 26 20 26 18 26 17 26 21 26 24 26 25 26 25 26
26 26 26 26 24 26 20 26 18 26 16 26 17 26 21 26 24 26 25 26 25 26
26 26 25 26 23 26 19 26 17 26 15 26 16 26 21 26 23 26 25 26 25 26
26 26 25 26 23 26 22 26 21 26 18 26 18 26 21 26 24 26 25 26 25 26
25 26 25 26 24 26 23 26 21 26 20 26 20 26 24 26 25 26 25 26 25 26
25 26 25 26 25 26 24 26 22 26 23 26 23 26 25 26 25 26 25 26 25 26
25 26 25 26 25 26 25 26 25 26 24 26 25 26 25 26 25 26 26 26 26 26
26 26 26 26 25 26 25 26 25 26 25 26 25 26 25 26 26 26 26 2  26
26 26 26 26 26 26 26 26 25 26 25 26 25 26 26 26 26 26 26 26 26
26 26 26 26 26 26 26 26 26 26 25 26 25 26 26 26 26 26 26 26 26
```

Fig. 13-8. Digitized topography for case 8, where every other NS row of the seamount Ryofu is assumed non-magnetic. Units are the same as in Fig. 13-1.

BASE LEVEL = 26

BATHYMETRY

```
26 26 26 26 26 26 26 25 25 26 26 26 25 26 26 26 26 26 26 26 26 26
26 26 26 26 26 26 26 26 26 26 26 26 26 26 26 26 26 26 26 26 26 26
26 26 26 25 25 25 24 24 23 23 25 24 23 23 24 25 25 25 26 26 26 26
26 26 26 26 26 26 26 26 26 26 26 26 26 26 26 26 26 26 26 26 26 26
26 26 26 25 25 24 22 22 21 21 21 20 19 20 22 24 25 25 25 25 25 26
26 26 26 26 26 26 26 26 26 26 26 26 26 26 26 26 26 26 26 26 26 26
26 26 26 25 24 23 20 19 18 17 16 16 17 20 21 22 24 25 25 25 25 25
26 26 26 26 26 26 26 26 26 26 26 26 26 26 26 26 26 26 26 26 26 26
26 25 25 24 23 23 22 22 21 19 18 17 18 20 21 23 24 25 25 25 25 25
26 26 26 26 26 26 26 26 26 26 26 26 26 26 26 26 26 26 26 26 26 26
25 25 25 25 25 24 24 23 22 23 23 22 23 24 25 25 25 25 25 25 25 25
26 26 26 26 26 26 26 26 26 26 26 26 26 26 26 26 26 26 26 26 26 26
26 26 26 26 25 25 25 25 25 25 25 25 25 25 25 25 26 26 26 26 26 26
26 26 26 26 26 26 26 26 26 26 26 26 26 26 26 26 26 26 26 26 26 26
26 26 26 26 26 26 26 26 26 26 25 25 25 26 26 26 26 26 26 26 26 26
```

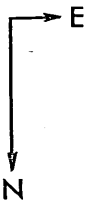

Fig. 13-9. Digitized topography for case 9, where every other EW row of the seamount Ryofu is assumed non-magnetic. Units are the same as in Fig. 13-1.

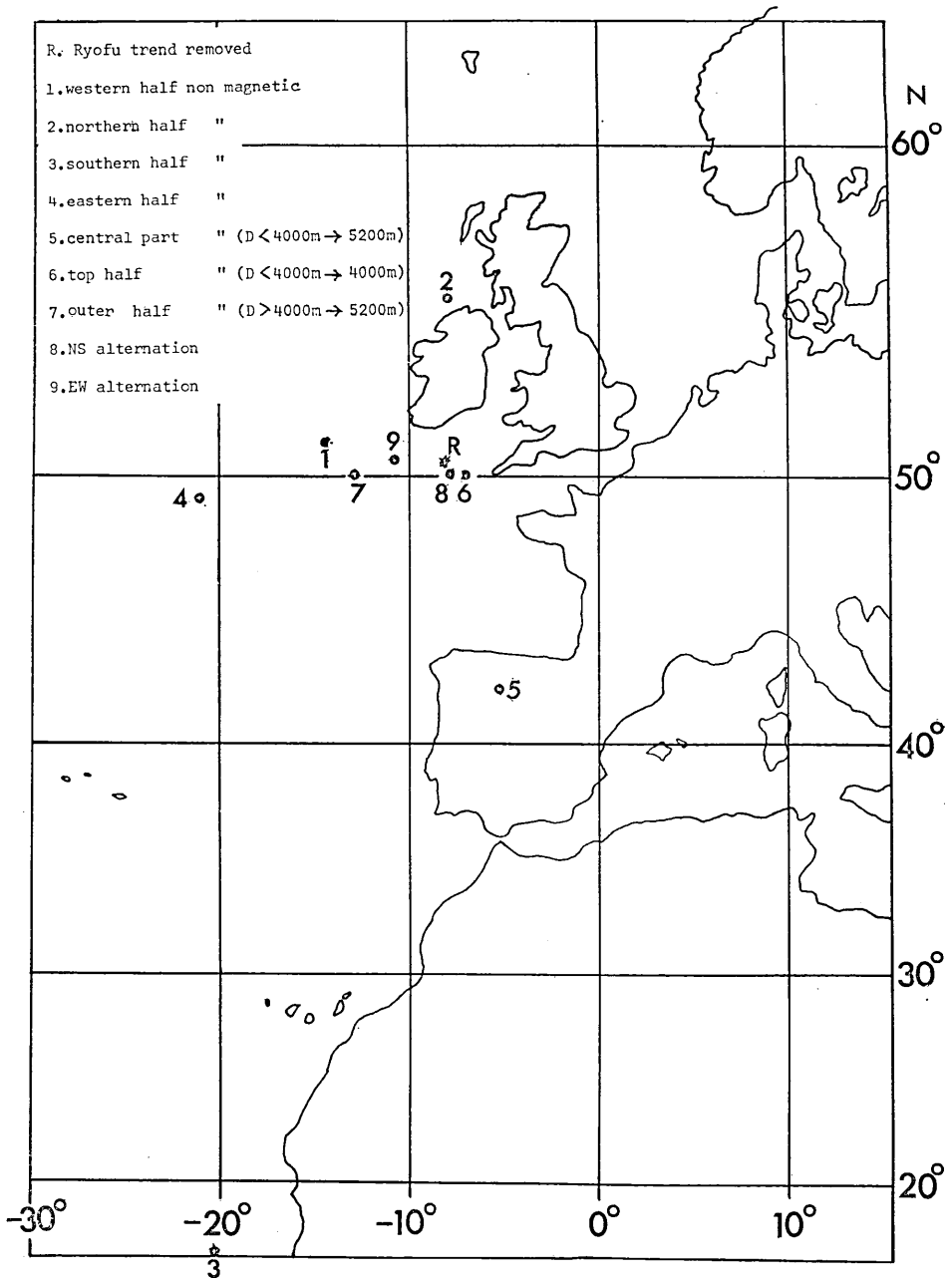

Fig. 14. Pole positions for the seamount Ryofu in cases 1-9. R is for the case of uniform magnetization.

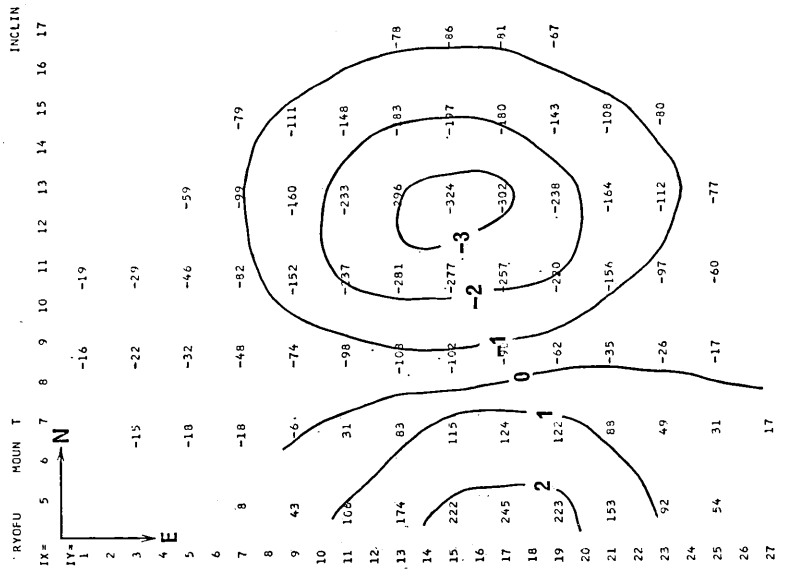

Fig. 15. The computed anomaly for the seamount Ryofu in case 6.

magnetizations are shown in Figs. 13-2~9. Among these cases 2~4 are evidently similar to case 1 explained above. In case 5, the central part of the seamount where the depth is less than 4000m (20 in our vertical unit) is supposed non-magnetic, in case 6, the part above 4000m depth is non-magnetic, and in case 7 the outer part of the seamount where the depth is greater than 4000m is non-magnetic. In cases 8 and 9, every other NS row and EW row in our digitized topographic units are assumed non-magnetic. The results of the experiments are shown in Table III and Fig. 14. The shift of pole position is not very serious except for case 3 where the southern half of the seamount is assumed non-magnetic. It may be worth noticing that the goodness ratio, R, for case 6, where the top half (depth less than 4000m) is assumed non-magnetic, is 3.36. This value is significantly higher than in other cases, including the case for uniform magnetization. This result may mean that the top part of the seamount is in fact magnetized much more weakly as compared with the lower part. Fig. 15 is the plot of the computed anomaly for case 6 to be compared with Figs. 11-a, and b. In any case, the computed effects appear not to be really serious in view of other uncertainties, so that in the following we tentatively take the case of uniform magnetization exclusively for the other seamounts.

In the calculation of pole positions, it was assumed that the magneti-

zation is entirely remanent. In fact, the seamount must have some induced magnetization in the direction of the present geomagnetic field. Effect of induced part of magnetization, however, can be assessed to some extent; one can assume the possible range in the magnitude of magnetic susceptibility and estimate the vector of remanent magnetization through simple vectorial subtraction, and then compute the corresponding pole position. The segments of the arcs in Fig. 12, show the variation of pole positions with the magnetic susceptibility; the northern end is for zero susceptibility, i.e. the magnetization is entirely remanent. *Kagami et al.* (1965) reports that Sisoev seamount is formed probably by olivine basalts, and olivine augite basalts. Although we have little direct evidence about the petrology of rocks forming other seamounts, it would seem reasonable to suppose that the rocks are basalts with the magnetic susceptibility ranging from 10^{-4} to 10^{-2} *emn/cc* (*Cox and Doell*, 1962; *Ade-Hall*, 1964). We can now compute the intensities of the remanent and induced magnetizations for each assumed susceptibility value and, from these values, compute the Königsberger ratio, Q, which is the ratio of remanent and induced magnetizations. The ends of arcs in Fig. 12 are for the Q-ratios of 2.0. It is now evident that as long as the Q-ratio is greater than say 2.0, the effect of induced magnetization is small for each case. The value of 2.0 is considered to be modest for basaltic volcanics. *Cox and Doell* (1962) and *Ade-Hall* (1964) both report that the Q-ratio of sub-marine basalts is usually greater than 10. If the Q-ratio of 10 is assumed, the true pole positions are almost indistinguishable from the case of the non-induced component in the figure. Allowance should be made for the fact, however, that the effective Q for seamounts may be less than that observed for small specimens, because of possible non-uniformity in the direction of remanent magnetization of the mountain bodies. The magnitudes of susceptibility corresponding to the case of $Q=2$ for seamounts A, Sisoev, B and Ryofu are roughly 1.4×10^{-2} *emu/cc*, 0.8×10^{-2} *emu/cc*, 0.4×10^{-2} *emu/cc* and 0.5×10^{-2} *emu/cc*. Discussion similar to the above was made by *Mason and Richardson* (1965) who also estimated the pole positions for a number of seamounts including the present ones. The data used by Mason and Richardson for the present seamount are the same as ours, but their method of computation is different from ours. They also found the pole positions to be in the North Atlantic though details have not yet been published.

The apparent palaeomagnetic colatitudes of these seamounts are 89° for seamount A, 78° for Sisoev, 92° for B and 89° for Ryofu, giving

the average of 87°. Therefore the seamounts were, apparently, nearly on the magnetic equator when magnetized.

As for the age of these seamounts, a type fossil (Nerinea) of Cretaceous age was sampled from the seamount Sisoev. (*Kagami et al.* 1965). According to these authors, it can be said that at least the seamount Sisoev was formed some time in the Mesozoic, and its top was above the sea level whereas it is now submerged to a depth of about 3700m.

Palaeomagnetism of the Cretaceous age in Japan is rather complex. Cretaceous virtual geomagnetic poles from red shale in southwestern Japan by *Nagata et al.* (1962) are in the east Pacific and these poles, being far from Cretaceous poles from other areas of the world, were interpreted as due to the clockwise rotation of Japan since the Cretaceous time. Pole position from a lava in northeastern Japan by these authors was located in North Africa or its antipodal position (*Ozima*, 1963). Recently *Fujiwara and Nagase* (1965) peport considerably scattered Cretaceous pole positions determined from basic rocks in Hokkaido. On the other hand, studies by *Kawai et al.* (1961) showed that the declination as well as inclination of rocks bear witness of a bending of the Japanese Island about 45° degrees. If we assume with these authors that southwestern Japan remained fixed and that northeastern Japan bent anticlockwise, this bendings might have been due to the stress indicated by the arrows in Fig. 12. Palaeomagnetic investigation for the Cretaceous age from other parts of the world as compiled by *Irving* (1964. p. 114) indicate some scatter.

If it is tentatively assumed that the polar wandering since the Cretaceous time was small and the true pole has remained in the proximity of the present geographic pole, the deviation of the poles for the present seamounts may be explained by the movements of the seamounts. Here, the idea of a spreading sea floor as developed by *Hess* (1962), *Dietz* (1962) and *Wilson* (1963) is somewhat suggestive. Wilson suggests that the movement of sea floor in the Pacific might be as shown by the arrows in Fig. 12, and that the linear alignment of the Hawaiian Islands is one of the results of the spreading of the sea floor. Our seamounts happen to be roughly on the extension of the array of the Hawaiian Islands. As mentioned earlier, palaeomagnetically the present seamounts were formed in the equatorial region. Since we have no control of palaeolongitude, we might be tempted to say that they drifted in the direction suggested by Wilson. Then, the intersection of the assumed path and the equator

is found roughly, as seen in Fig. 12, where the East Pacific Rise, the postulated source area of the spreading Pacific floor, intersects the equator. If we draw a great circle path through the seamounts and the Hawaiian Islands, it crosses the equator about 30° west of the intersection of the East Pacific Rise and the equator. But such a discrepancy is immaterial in the present discussion. The picture suggested here is extremely speculative and definitely premature. It is not in harmony with Wilson's idea about the Hawaiian Islands, where the source of volcanic activity is supposed to have existed under the present main Island of Hawaii. In the above discussion, possible movement of the seamounts was considered in the framework of the *bold* hypothesis (*Menard*, 1965) of sea floor spreading. The relation of the proposed path and the Darwin Rise (*Menard*, 1965), for instance, should await further data.

Richards, Vacquier and van Voorhis (1965) computed the magnetization of seamounts and volcanoes, including nine seamounts southwest of the Hawaiian Islands. Palaeomagnetic pole positions of these "Hawaiian" seamounts are plotted in Fig. 12 for comparison. It may be observed that, except for one pole in Siberia, the grouping of the pole positions is almost as good as that for the Japanese seamounts. The average palaeomagnetic colatidude of the "Hawaiian" seamounts is about 100°, indicating that these seamounts were formed at about 10° south of the equator. Again these seamounts may be suspected to have travelled along more or less in the same manner as the Japanese seamounts. The age of one seamount belonging to the "Hawaiian" group was measured as 85 ± 2 million years by the $K-Ar$ method on a dredged rock sample (Vacquier, private communication).

Naturally, there are many details that have to be clarified before anything definite could be stated regarding the significance of these results, but still it appears to be noteworthy that the grouping of the pole positions inferred from seamount is as good as, if not better than, the more usual palaeomagnetic pole positions. As long as the assumption of the dipolar nature of the geomagnetic field is maintained and the time required for the formation of the seamounts was long compared with the time required to average out the secular variations, the observed clustered seamount pole positions should represent a part of another meaningful polar wandering path: *polar path from the Pacific*. It is possible, if not probable, that the poles really indicate the wandering of the pole and not the displacement of the seamounts. In that case, the usual Cretaceous palaeomagnetic poles from continents, most of which

are on the other side of the present pole (*Irving*, 1964, Fig. 6.7.), should be explained by the drift of continent relative to the Pacific seamounts. We need much more data.

In conclusion, therefore, we would like to emphasize, with *Mason and Richardson* (1965), that the palaeomagnetic study of numerous seamounts existing all over the ocean bottom may bring about some significant contribution toward the clarification of many important problems about the origin and history of the oceans and continents. Again, much more work is undoubtedly necessary before anything definite can be postulated.

Acknowledgement

The authors would like to thank Prof. Victor Vacquier for his help in the programming of the computation. They appreciate the kind cooperation of Dr. Roger Miller, Computation Center, Stanford University. The computation was supported by this Computation Center. Miss T. Tanaka and Y. Kawakami are acknowledged for their help in the preparation of the manuscript and diagrams.

References

ADE-HALL, J. M., The magnetic properties of some submarine oceanic lavas, *Geophys. J.*, **9**, 85-92, 1964.

COX, A and R. R. DOELL, Magnetic properties of the basalt in Hole EM 7, Mohole Project, *J. Geophys. Res.*, **67**, 3997-4004, 1962.

DIETZ, R., Ocean-basin evolution by sea-floor spreading, in *Continental Drift*, Ed. by S. K. Runcorn., Academic Press, 1962.

FUJIWARA, Y and M. NAGASE, Palaeomagnetic Studies of the Cretaceous rocks in the Nemuro Peninsula, Hokkaido, Japan, *"Earth Science" (Chikyu Kagaku), Jour. of Assoc. for Geol. Collaboration in Japan*, No. 79, 42-46, 1965.

IRVING, E., *Palaeomagnetism*, (Wiley, 1964).

HESS, H. H., History of Ocean basins, in *Petrologic Studies*, A volume in Honor of A. F. Buddington, Ed. by A. E. J. Engel, H.L. James and B. L. Leonard, Geol. Soc. Amer., New York, 1962.

KAGAMI, H., T. SATO, K. OSHIDE, J. ISHII, R. TSUCHI, H. MII, K. KOIZUMI, H. SHIOZAWA, M. NOGAMI, Japan Trench survey by R. V. Ryofu-Maru (JEDS-6, 1963), *Chishitsugaku Zasshi*, 71, 414, 1965 (Abstract in Japanese only).

KAWAI, N, H ITO and S. KUME, Deformation of the Japanese Islands as inferred from rock magnetism, *Geophys. J.*, **6**, 124-130, 1961.

MASON, R. G. and A. RICHARDSON, Palaeomagnetic significance of the magnetic fields of seamounts, *Trans. Amer. Geophys. Union*, **46**, 68, 1965 (Abstract only).

MENARD, H. W., Sea floor relief and mantle convection, *Phys. and Chem. of the Earth*,

6, 315-364, 1965.

NAGATA, T., S. AKIMOTO, Y. SHIMIZU, K. KOBAYASHI and H. KUNO, Palaeomagnetic studies on Tertiary and Cretaceous rocks in Japan, *Proc. Japan Acad.* **35**, 378-383, 1959.

OZIMA, M., Review of Palaeomagnetic study at Geophysical Institute, University of Tokyo, *"Earth Science"* (*Chiku Kagaku*), *J. of Assoc. for Geol. Collaboration in Japan*, No. 65, 20-23, 1963.

RICHARDS, M., V. VACQUIER and G. VAN VOORHIS, private communication, to be published in *Geophysics*, 1965.

UYEDA, S., T. SATO, M. YASUI, T. YABU, Y. WATANABE, K. KAWADA and Y. HAGIWARA, Report on geomagnetic survey in the northwestern Pacific during JEDS-VII and JEDS-VIII cruises., *Bull. Earthq. Res. Inst.*, **42**, 555-570, 1964.

UYEDA, S., M. YASUI, K. HORAI and Y. YABU, Report on geomagnetic survey during JEDS-4 cruise, *Oceanogr. Mag.*, **13**, 167-183, 1962.

VACQUIER, V., A machine method for computing the magnitude and the direction of magnetization of a uniformly magnetized body from its shape and a magnetic survey, *Proc. Benedum Earth Magnetism Symposium.*, Pittsburgh, 123-137, 1962.

---

11. 日本列島沖の4個の海山の磁化について

地震研究所 上田誠也

スクリプス海洋研究所 Michael RICHARDS

本州東北部および北海道沖の太平洋に存在する4個の海山について，その測深結果および，磁気測量（プロトン磁力計による全磁力）結果にもとづき，磁化方向，強度を推定した．推定にはVacquierの方法を用い，計算はスタンフォード大学のIBM 7090によつて行なわれた．海山はいづれも現在の地球磁場に比べて順方向に帯磁しているが，伏角はいづれも小さく，上向きの場合もあることが結論された．磁化は残留磁化が主成分と考えられるので，この結果にもとずき，古地磁気学的磁極を計算すると，大西洋北部に比較的よく集中する．これらの海山の生成年代は中生代と考えられるので，ここに得られた結果は，太平洋底の移動によるものかもしれない．但し，その可能性を確めるには，更に多くの海山について同様の研究を行うことが必要である．